PACIFIC EARTHQUAKE ENGINEERING RESEARCH CENTER

Calibration of Semi-Stochastic Procedure for Simulating High-Frequency Ground Motions

Jonathan P. Stewart

Emel Seyhan

Department of Civil and Environmental Engineering
University of California, Los Angeles

Robert W. Graves

U.S. Geological Survey, Pasadena, California

PEER 2011/09
DECEMBER 2011

Disclaimer

The opinions, findings, and conclusions or recommendations expressed in this publication are those of the author(s) and do not necessarily reflect the views of the study sponsor(s) or the Pacific Earthquake Engineering Research Center.

Calibration of Semi-Stochastic Procedure for Simulating High-Frequency Ground Motions

Jonathan P. Stewart
Emel Seyhan
Department of Civil and Environmental Engineering
University of California, Los Angeles

Robert W. Graves
U.S. Geological Survey, Pasadena, California

PEER Report 2011/09
Pacific Earthquake Engineering Research Center
College of Engineering
University of California, Berkeley

December 2011

ABSTRACT

Broadband ground motion simulation procedures typically utilize physics-based modeling of source and path effects at low frequencies coupled with semi-stochastic procedures at high frequencies. The high-frequency procedure considered here combines a deterministic Fourier amplitude spectrum that is a function of closed-form source, path, and site models with a random phase. Previous analysis of the simulation procedure in the ShakeOut exercise demonstrated faster distance attenuation and lower intra-event dispersion of high-frequency ground motions than in empirical ground motion equations. We increase crustal damping (*Q*) to remove the distance attenuation bias and introduce random site-to-site variations to the Fourier amplitudes using a log-normal standard deviation ranging from 0.45 for $M_w < 7$ to zero for M_w 8. We repeat the simulation of the ShakeOut event with the increased crustal damping and a revised source characterization, with increased slip heterogeneity reflecting more recent recommendations. The revised simulation procedure for ShakeOut produced ground motions without a distance attenuation bias and with near-source dispersion that is generally compatible with empirical models. However, far-field dispersion remains lower than empirical models.

ACKNOWLEDGMENTS

This work was supported by the State of California through the Transportation Systems Research Program of the Pacific Earthquake Engineering Research Center (PEER) under award number SA#6924. The third author was partially supported by a grant from the Southern California Earthquake Center (SCEC). The repeat of the large-scale ShakeOut simulation was run at the Center for High-Performance Computing and Communications (http://www.usc.edu/hpcc) at the University of Southern California under an agreement with the SCEC CME project. Any opinions, findings, and conclusions or recommendations expressed in this material are those of the authors and do not necessarily reflect those of the National Science Foundation, U.S. Geological Survey, or PEER. We would like to express our gratitude to Ken W. Hudnut and David M. Boore for their constructive and insightful review comments.

CONTENTS

LIST OF TABLES AND FIGURES

1 Overview of the Study

1.1 INTRODUCTION

Broadband simulation procedures have the potential to play a significant role in the engineering characterization of seismic ground motion, especially for conditions poorly represented in ground motion databases. For example, the database used in the Next Generation Attenuation (NGA) project included earthquake magnitudes up to M_w 7.9, but recordings at moderate to close distances (< 40 km) for M_w > 7.6 are relatively sparse [Chiou et al. 2008]. Ground motion hazard studies for sites in the vicinity of the San Andreas fault are often controlled by earthquake magnitudes near 8.0, e.g., Harmsen and Frankel [2001]. There is significant practical need for ground motion prediction tools that can operate beyond the limits of the database. Broadband simulations have the potential to help solve two important problems by providing: (1) simulated motions to help constrain semi-empirical ground motion prediction equations (GMPEs) beyond the data limits; and (2) realistic waveforms for use in response history analyses for conditions not represented in empirical databases.

Ground motion simulation procedures vary in their methodology and sophistication, but all compute in some manner source processes, path effects, and local site response. Deterministic procedures utilize rigorous seismological models of source, path, and site response without introducing a stochastic element. Such procedures are typically useful only at frequencies below about 1 Hz (e.g., Frankel [1993]; Sato et al. [1999]; Stidham et al. [1999]; Xu et al. [2003]; Day et al. [2008]; Olsen et al. [2008, 2009]). Higher frequency seismic waveforms are difficult to reproduce deterministically, in part because source radiation and wave propagation become increasingly incoherent at high frequencies (e.g., Liu and Helmberger [1985]; Sato and Fehler, [1998]; Hartzell et al. [1999]). Motions lacking coherency are by definition stochastic; accordingly, a separate family of non-deterministic simulation procedures has been used for many years that employ stochastic components (referred to here as "semi-stochastic"; see Boore,

[1983]; Silva and Darragh [1995]; and Beresnev and Atkinson [1997], Ameri et al., [2009]) or which are more fully stochastic (e.g., the non-stationary models of Conte and Peng [1997] or Rezaeian and Der Kiureghian [2008]).

Hybrid ground motion simulations leverage the strengths of deterministic procedures at low frequencies and stochastic or semi-stochastic procedures at higher frequencies to produce broadband waveforms. For a review of past hybrid methods, see Hartzell et al. [1999], Liu et al. [2006], Graves and Pitarka [2010], and Mena et al. [2010]; the latter two references present recent developments in two alternative hybrid procedures. Most modern broadband procedures use analytical Green's functions to model low-frequency path effects, including the effects of sedimentary basins. Current procedures are differentiated principally in the following respects:

1. The source description for low-frequency simulations is described kinematically (including spatially variable slip distributions, rise times, and rupture velocities) or is represented through spontaneous dynamic processes (which prescribe initial fault stresses and constitutive relations for shear failure criteria). In some cases, the development of kinematic models is guided by results of dynamic rupture simulations [Guatteri et al. 2004; Schmedes et al. 2010], so the outcomes of the different modeling procedures can be similar. The kinematic approach is used by Liu et al. [2006], Frankel [2009], and Graves and Pitarka [2010]. A combination of kinematic and dynamic rupture modeling was considered by Hartzell et al. [2005] and Mena et al. [2010]. The dynamic rupture approach is used by Pulido and Dalguer [2009] and Olsen et al. [2008; 2009].

2. High-frequency source and path effects are simulated semi-stochastically (as described below) or deterministic methods are applied in which random processes are introduced through the source description or path operators. The semi-stochastic approach prescribes the Fourier amplitude using a deterministic mean combined with random frequency-to-frequency perturbations, whereas the phase is stochastic (e.g., Hartzell et al. [1999; 2005]; Frankel [2009]; Graves and Pitarka [2010]). Mai et al. [2010] and Mena et al. [2010] introduce stochasticity through scattering operators within the analytical Green's functions, which requires tuning of scattering parameters and inherently takes high-frequency incoherence as predominantly path-

induced. Liu et al. [2006] introduce stochasticity via the source, which is defined to very short length scales with variable slip, rise times, and rupture velocities.

Because ground motion simulation involves complex numerical models with significant potential for coding errors, simulation results should be verified by comparing outcomes (at low frequencies) from independent computational platforms for a common set of source and path conditions [Bielak et al. 2010]. Such verification is an essential first step towards the establishment of simulation procedures as a potentially reliable engineering tool. Following verification, careful validation and calibration of simulation results relative to ground motion data or data-driven empirical models is necessary. The lack of engineering application of broadband simulations in the western United States to date reflects, in part, the lack of validation and calibration to convince engineers of the reliability of simulation tools. In general, the following procedures have been used for validation/calibration:

Waveform comparisons using earthquake data: Simulated waveforms for a particular earthquake event are compared to recordings (e.g., Zeng et al. [1994]; Stidham et al. [1999]; Hartzell et al. [2005]; Liu et al. [2006]; Graves and Pitarka [2010]; Mai et al. [2010]). In most cases these comparisons are qualitative, however, quantitative comparison schemes have also recently been proposed (e.g., Olsen and Mayhew [2010]). Qualitative waveform comparisons are the most common validation technique in previous research. Typically, velocity or displacement histories are used for these comparisons that emphasize low-frequency ground motions relatively unaffected by stochastic processes. Potential issues with this approach are (1) often the same recordings used to invert the source function are then used to demonstrate the efficacy of the simulation code, which makes good matches probable but less meaningful; and (2) high-frequency components are often not considered.

Ground motion intensity measures comparison using earthquake data: Intensity measures (IMs), such as peak velocity or spectral quantities, are calculated for simulated motions from an event and compared (as a function of distance or frequency) to IMs from recordings (e.g., Silva et al. [1999]; Hartzell et al. [1999; 2005]; Liu et al. [2006]; Graves and Pitarka [2010]; Mai et al. [2010]). If a suitable number of recordings are available, both bias and dispersion of simulated motions can be compared to those obtained from recordings. One drawback of this approach is that recordings are generally not available for the types of earthquakes for which simulations are most valuable (i.e., large magnitude). In addition, the circular reasoning associated with use of an inverted source function with recordings from that same event (as described above) diminishes the value of these comparisons.

Ground motion IM comparison using prediction equations: Ground motions are simulated for hypothetical events and IMs are compared to predictions from semi-empirical Ground Motion Prediction Equations (GMPEs). This approach enables relatively robust evaluations of distance scaling, site response, and standard deviation terms (e.g., Star et al. [2011]) or subsets of these terms [Frankel 2009]. Parameters in the simulation code can be calibrated to match GMPE trends; for example, Mena et al. [2010] calibrated the number of scatterers to achieve desired median levels of high-frequency motions in their hybrid procedure.

Most of the procedures described above *validate* simulations in the sense that computed motions (or their IMs) are simply checked against data or GMPEs—although we expect that some process of parameter adjustment (i.e., informal calibration) has typically been undertaken to fit simulation results to data in a generalized sense. Relatively formal *calibration* involves adjusting model parameters to achieve specified attributes in simulated motions. As a first step of the calibration process, we describe calibration of selected high-frequency components of the broadband simulation procedure of Graves and Pitarka [2010]. The calibration seeks to remove too-fast distance attenuation in simulated motions and too-low standard deviation terms. Previous work by Star et al. [2011] identified these problems with broadband simulated motions using motions from a ShakeOut (southern San Andreas fault) earthquake (e.g., Graves et al., [2008] and Porter et al. [2011]). Calibration of low-frequency components is not undertaken in the work reported herein.

Following this introduction, we briefly review the hybrid broadband simulation methodology that is the subject of this work, with an emphasis on the high-frequency (semi-stochastic) component. We then describe a series of hypothetical events for which high-frequency ground motions are simulated Using the ShakeOut rupture scenario [Graves et al. 2011], we demonstrate that the short-period IMs of ground motions generated using the high-frequency simulation procedure are similar to broadband motions with respect to their distance attenuation and dispersion. We then calibrate the simulation procedure by (1) modifying the crustal damping (Q model) to remove distance attenuation bias relative to NGA GMPEs; and (2) adding dispersion to match intra-event standard deviations in GMPEs. We conclude by repeating the ShakeOut broadband simulations using the modified hybrid procedure.

2 Utilized Simulation Methodology

We utilized the hybrid broadband simulation methodology of Graves and Pitarka [2010] This method was selected from among several hybrid simulation procedures principally on the basis of its utilization in high-profile scenario earthquake and loss estimation studies (e.g., Aagaard et al. [2008]; Graves et al. [2011]). The Graves and Pitarka [2010] procedure consists of a low-frequency component that utilizes a kinematic source model and analytical Green's functions for path effects. This low-frequency portion of the model is not the subject of this work.

The high-frequency portion of the model is adapted from the classical point source simulation procedure of Boore [1983], later adapted to finite sources by Frankel [1995]. The source and path components for a finite fault are summed as follows to construct the Fourier spectrum for a given site:

$$A(f) = \sum_{i=1}^{N} \sum_{j=1}^{M} C_{ij} \bar{S}_i(f) G_{ij}(f) P(f) \tag{2.1}$$

Spectrum $A(f)$ would apply at the location of interest if the site condition matched that at the top of the crustal velocity model, which is moderately hard rock (V_{s30} = 865 m/sec). Modifications to other site conditions were made using the nonlinear site amplification factors used in the Campbell and Bozorgnia [2008] GMPE, which utilize V_{s30} and peak acceleration on a reference rock site condition with a reference V_{s30} of 1100 m/sec. The simulated motions are modified from 865 m/sec to the reference V_{s30} of 1100 m/sec (using the Campbell and Bozorgnia site factors) before application of the V_{s30}-dependent site factor. The fault is discretized into i=1 to N sub-faults, each with its own prescribed slip δ_i. Seismic waves can travel from the source along j=1 to M ray paths (e.g., two are used by Graves and Pitarka, [2010]; direct and Moho-reflected). The source spectrum for sub-fault i and ray path j includes (1) a frequency-independent term (C_{ij}) that accounts for radiation pattern as well as shear wave velocity and mass density of rock at the sub-fault and (2) a frequency-dependent term $S_i(f)$ that describes the seismic radiation from sub-fault i.

As shown schematically in Figure 2.1, the source spectrum $C_{ij}\ S_i(f)$ is broad banded with an ascending branch that scales with the square of frequency and a flat branch for frequencies beyond the corner frequency f_{ci}. Additional parameters affecting source term $S_i(f)$ include the moment release on sub-fault i, rupture velocity, and stress parameter (σ_p), and are discussed in detail by Graves and Pitarka [2010].

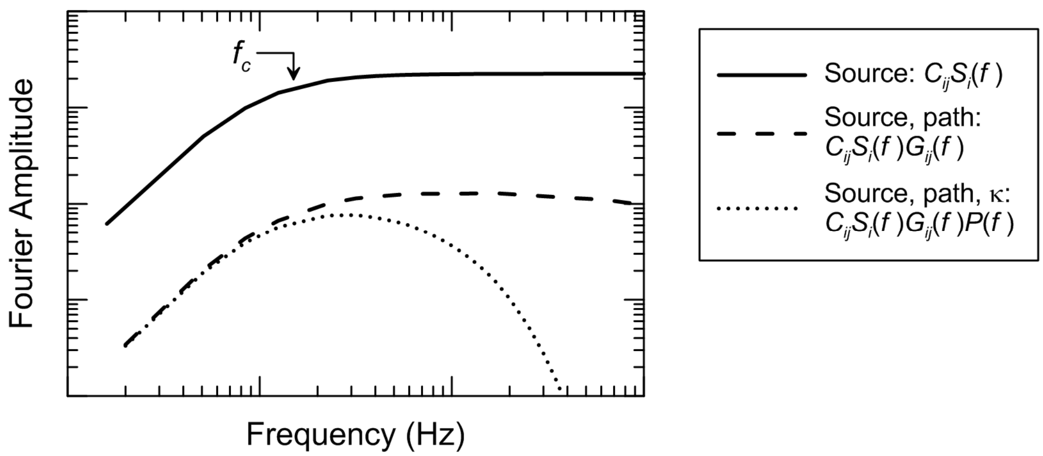

Figure 2.1. Schematic illustration of source term, path operator, and effect of κ on Fourier amplitude spectrum. The spectra depicted are smooth mean curves. White noise perturbations from the mean are applied for a given site according to the procedure described in Boore [1983].

The path parameter $G_{ij}(f)$ is calculated as:

$$G_{ij}(f)=\frac{I_i(f)}{R_{ij}}\exp\left[-\pi f\sum_{k=1}^{L}\frac{\Delta t_k}{Q_k(f)}\right] \tag{2.2}$$

where R_{ij} represents ray path distance from sub-fault i to the site along path j (i.e. path length), $I_i(f)$ represents impedance effects calculated using quarter wavelength theory [Boore and Joyner 1997] that uses a crustal velocity model specified across k=1 to L layers having thickness Δz_k, shear wave velocity V_{sk}, and path attenuation term Q_k. Early methods used $1/R$ (R is the distance from source to site) to approximate the distance attenuation (geometric spreading) of high-frequency body waves [Boore 1983]. Clearly this does not apply for longer periods or situations where surface waves become more important, and more recent applications utilize a geometric spreading term of the form $1/R^x$, where ^{x} can be a function of distance and frequency to account for these complexities (e.g., Atkinson et al. [2009]). In Equation (2.2), $1/R_{ij}$ corresponds to 1/path length, which is close to $1/R$ for a direct ray path. For a reflected ray path, the value of $1/R_{ij}$ is reduced due to the longer ray path. However, the full response at a particular site represents a summation over multiple ray paths, which can add constructively when several rays arrive at the site at approximately the same time. Assuming sufficient rays are considered, this approach naturally incorporates velocity model specific variations in geometric spreading due to crustal reflections and development of surface waves [Graves and Pitarka 2010]. The term Δt_k represents travel time through layer k and is equal to $\Delta z_k /(V_s)_k$ for vertically propagating waves. As shown in Figure 2.1, the path term $G_{ij}(f)$ reduces ground motions relative to the source spectrum, with the amount of reduction increasing with frequency.

Figure 2.2(a) shows location-specific and generic crustal velocity models. The Northridge model utilized by Graves and Pitarka [2010] ranges from 3.8 km/sec at 31 km depth to 0.45 km/sec at the surface with a V_{s30}=865 m/sec. The path attenuation term depends on the shear wave velocity of each layer and frequency as follows:

$$Q_z(f) = Q_0 f^x = \left[a + bV_{s,z}\right] f^x \tag{2.3}$$

where a, b, and x are empirical parameters generally taken as 25, 34, and 0.6 to 0.8, respectively (e.g., Aagaard et al. [2008]; Graves and Pitarka [2010]). As shown in Figure 2.2(b), these parameters are generally consistent with Q models in past work (e.g., Raoof et al. [1999]; Fatehi and Herrmann [2008]). We acknowledge the implementation of Q can be somewhat different for these various models, particularly since a trade-off exists between the assumed geometric spreading term and the derived Q model. For the comparison shown here, we assume the geometric spreading to be constant for all models, which is most appropriate for near-source distances where the direct ray is dominant.

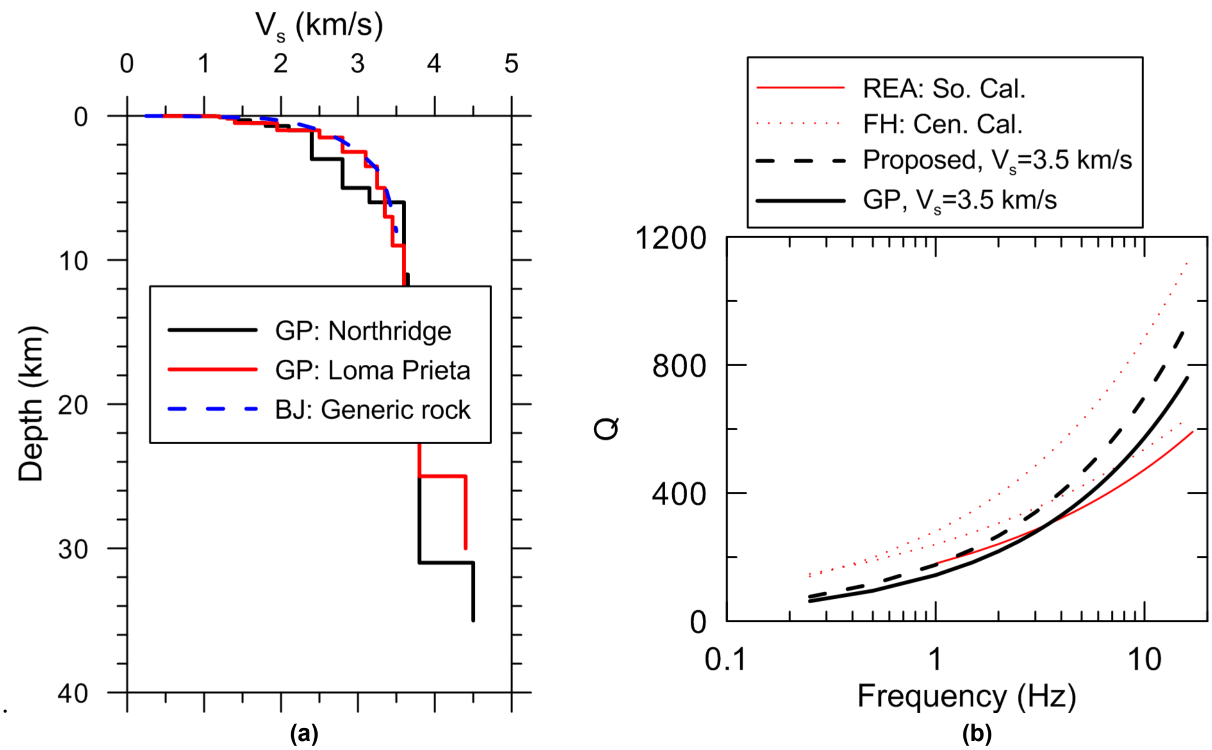

Figure 2.2 **(a) Crustal velocity models used by Graves and Pitarka [2010] for verifications of Northridge and Loma Prieta data and generic rock profile of Boore and Joyner [1997]; and (b) crustal *Q* models from Raoof et al. [1999] and Fatehi and Herrmann [2008] compared with default model from Graves and Pitarka [2010] and proposed adjustment presented herein.**

The term *P*(*f*) is a site term for modeling high frequency decay using the empirical κ_0 parameter (Anderson and Hough, [1984]):

$$P(f) = \exp(-\pi\kappa_0 f) \tag{2.4}$$

which is independent of distance in this formulation. Campbell [2009] presents typical values of κ_0, which was taken as 0.04 sec by Graves et al. [2011]. The effect of κ_0 on the Fourier spectrum is shown in Figure 2.1.

Each element of the high-frequency simulation procedure described to this point is theoretically-based and deterministic, in the sense that specified equations are used to represent modeled phenomena. However, there are stochastic elements to the simulations that affect the Fourier amplitude and phase. Two sources of randomness affecting amplitude are (1) random frequency-to-frequency perturbations applied to the smooth mean spectra shown in Figure 2.1, and (2) spatially variable slip among the subfaults (described below). The Fourier phase is taken from white noise. The random amplitude and phase perturbations are assumed to be uncorrelated between different frequencies and between sites for any particular frequency. Following the formulation of Boore [1983], the stochastic elements are introduced to the subfault source term $S_i(f)$ by including a windowed time sequence of band-limited random white Gaussian noise with zero expected mean and variance chosen to give unit spectral amplitude on the average. In addition, the response for each subfault is delayed in time to account for rupture propagation across the fault and the travel time of the given ray. The resulting source term is complex valued (i.e., it includes amplitude and phase) and is denoted $\bar{S}_i\left(f\right)$.

Figure 2.3 shows an example of high- and low-frequency waveforms and Fourier spectra from the broadband ShakeOut simulations of Graves et al. [2011]. The final simulated waveform was obtained by combining the low- and high-frequency results using a set of matched Butterworth filters that do not alter the phase of the response and sum to unity at all frequencies. These filters have already been applied to the high- and low-frequency motions plotted in Figure 2.4, with the crossover of the filters occurring at 1 Hz. Waveforms and spectra from the combined motions are also shown in Figure 2.4.

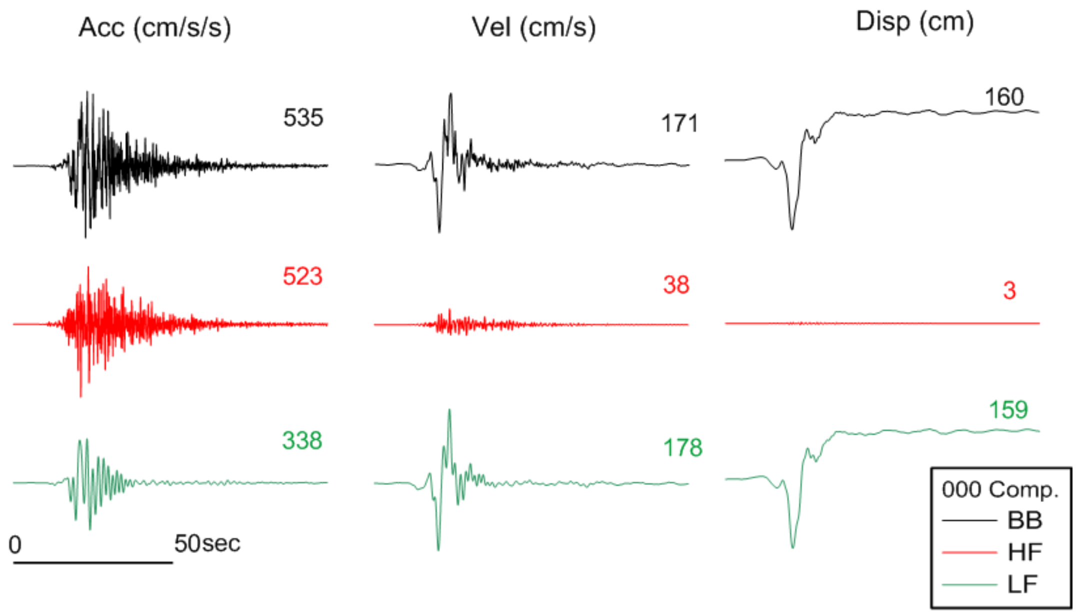

(a)

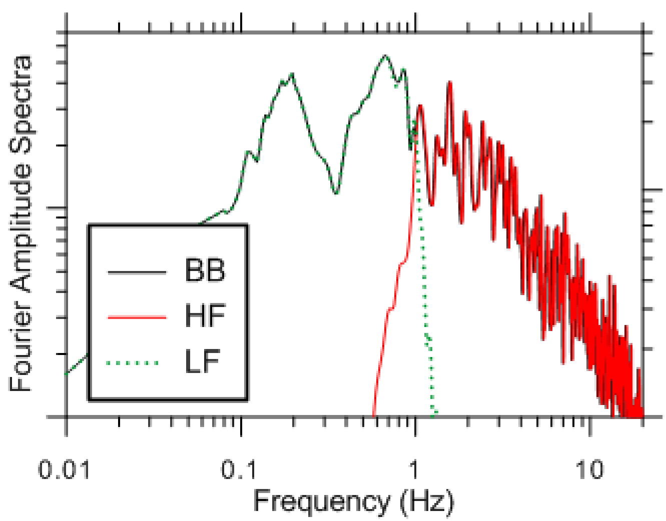

(b)

Figure 2.3 **(a) Acceleration, velocity, and displacement histories generated for M_w7.8 ShakeOut event at site HLN, which is about 5 km from the San Andreas fault in the San Bernardino region. Results from the high-frequency (HF) and low-frequency (LF) simulations are shown along with the full broadband (BB) motion; and (b) Fourier amplitude spectra of BB, HF, and LF acceleration histories from (a).**

3 High-Frequency Simulations for Parameter Calibration

3.1 CONDITIONS CONSIDERED

The simulated events are strike-slip earthquakes at four magnitudes (5.0, 6.5, 7.25, and 8.0). As shown in Figure 3.1, there are two events per magnitude having different slip distributions (but the same moment). The faults are vertically dipping and the rupture is bilateral with the epicenter at the middle of the fault. Additional details on the simulated fault ruptures are given in Table 3.1. The spatial variability of slip incorporates randomness and spatial correlation (see Graves and Pitarka [2010]). The level of slip randomness and spatial correlation affects ground motion dispersion; for the present application it was set at the levels described in Graves and Pitarka (2010), which is less smooth than the source models used in some previous applications such as ShakeOut [Graves et al. 2011].

The locations of simulated motions relative to the source faults are shown in Figure 3.2. Each array has recordings on lines radiating out from the fault. On each radiating line there are 18 stations at the following distances from the surface projection of the fault: 1.0, 1.5, 2.0, 3.0, 5.0, 7.0, 10, 15, 20, 30, 50, 70, 100, 120, 140, 160, 180, and 200 km.

Table 3.1 Attributes of simulated events for high-frequency ground motion simulations.

M_w	***Length (km)***	***Width (km)***	***Top Depth (km)***	***Subfault Size (km x km)***
5	3	3	10	1 x 1
6.5	26	12	0	2 x 2
7.25	102	18	0	3 x 2
8	416	24	0	4 x 3

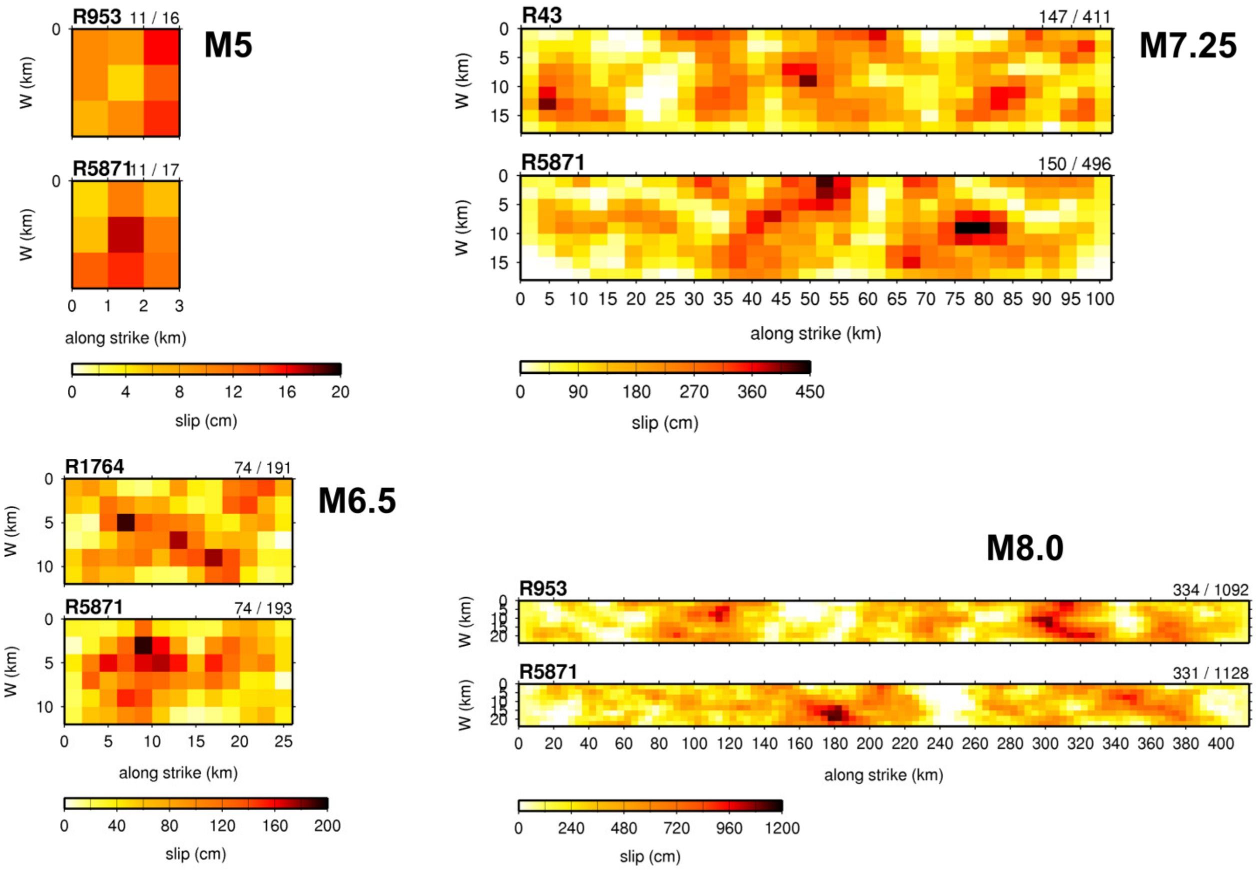

Figure 3.1 Slip models for M_w 5.0, M_w 6.5, M_w 7.25, and M_w 8.0 scenario earthquakes (from left to right).

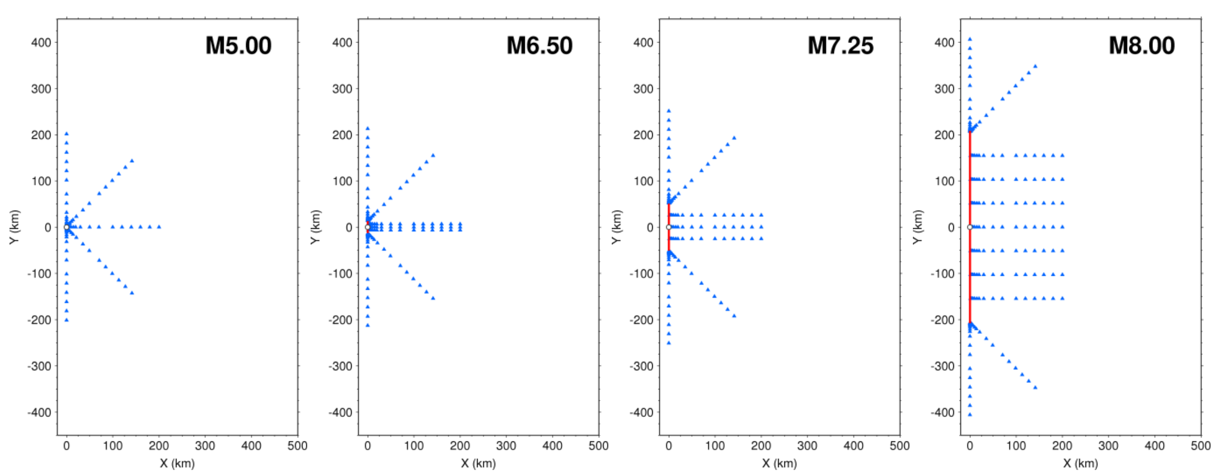

Figure 3.2 Station arrays for the four simulated strike-slip earthquakes. The red line indicates the fault.

3.2 COMPARISON OF MOTIONS FROM HIGH-FREQUENCY AND BROADBAND SIMULATIONS

The high-frequency simulation procedure utilized for the strike slip earthquakes depicted in Figures 3.1 and 3.2 is first applied to the ShakeOut source model [Graves et al. 2011] to investigate the relationship between short-period IMs from high-frequency and broadband simulations. Figure 3.3 shows the variation of PGA and 0.1, 0.3, and 1 sec pseudo-spectral accelerations (5% damping) with distance from the broadband simulations along with medians (μ) and medians ± two log standard deviations for data within distance bins. The binned quantities are also shown for the high-frequency simulations. The median and dispersion trends from the two data sets are similar, indicating that the high-frequency component of the simulation procedure has a dominant effect on each of the considered IMs. This finding supports focusing the calibration process on the high-frequency component of the simulation procedure to remove biases in simulated short-period IMs.

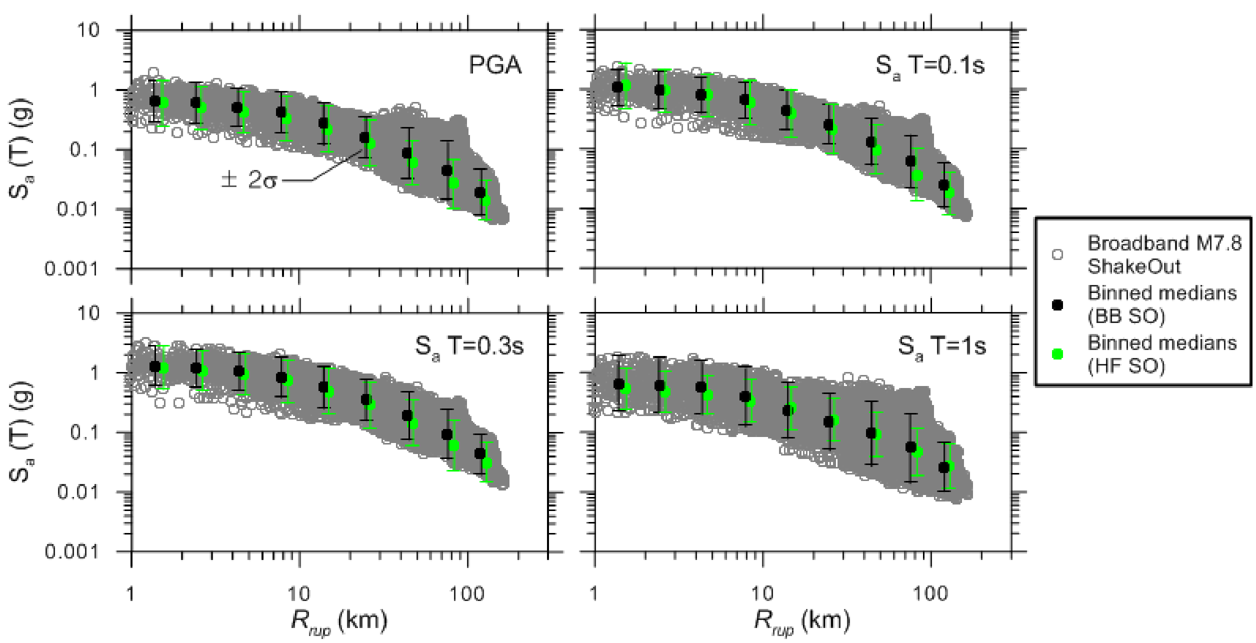

Figure 3.3 Spectral acceleration at 0.01 sec (PGA), 0.1 sec, 0.3 sec, and 1 sec from ShakeOut simulation using full broadband (BB) waveforms and high-frequency waveforms.

Star et al. [2011] found that high-frequency IMs from the ShakeOut broadband simulations attenuated faster with distance than suggested by the NGA GMPEs. This was found by calculating residuals between each simulated motion (treated like data) and the median model prediction from a GMPE as follows:

$$R_i(T) = \ln\left(S_a(T)\right)_{sim,i} - \ln\left(S_a(T)\right)_{GMPE,i} \tag{3.1}$$

where index i refers to a particular location where ground motions were simulated (latitude and longitude), $S_a(T)_{sim,i}$ refers to the 5% damped spectral acceleration of the simulated motion for oscillator period T at location i, $S_a(T)_{GMPE,i}$ refers to the median spectral acceleration for location i predicted by a GMPE considering the earthquake magnitude, site-source distance, and site condition, and R_i is the residual in natural logarithmic units. Residuals were calculated relative to the Abrahamson and Silva [2008], Boore and Atkinson [2008], Campbell and Bozorgnia [2008], and Chiou and Youngs [2008] GMPEs (referred to subsequently as AS, BA, CB, and CY).

Star et al. [2011] found residuals $R_i(T)$ to have a statistically significant slope with respect to rupture distance (R_{rup}) for the ShakeOut event for response spectral accelerations at periods under 5 sec. Using both the high-frequency and broadband simulations, we calculated values of $R_i(T)$ within distance bins as follows:

$$\overline{R}_k(T) = median\ \left[R_i(T)\right]_{i=1..N_k} \tag{3.2}$$

where k is an index for a particular distance bin having N_k simulated motions. As shown in Figure 3.4, distance attenuation trends were investigated by plotting $\overline{R}_k(T)$ for the two sets of simulations (broadband and high frequency only). As shown in Figure 3.3 for the 0.3 sec spectral acceleration and the BA GMPE, the slopes are similar for the broadband and high-frequency simulations. Similar results are obtained at other periods. These results verify that the high-frequency simulations reproduce the trends from broadband simulations that we seek to adjust through calibration. We undertake this in the following section.

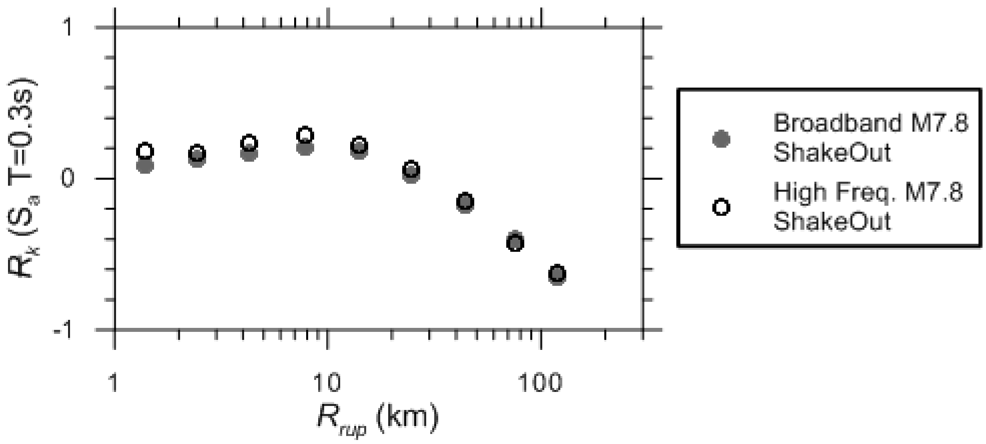

Figure 3.4 Median residuals of simulated motions (0.3 sec Sa) for Mw7.8 ShakeOut event from broadband procedure and its high-frequency component. The similarity of the slope of residuals with distance demonstrates that the high frequency component of the simulation procedure is responsible for the distance attenuation trend. Residuals calculated with respect to Boore and Atkinson [2008] (BA) GMPE.

4 Simulation Calibration

4.1 CALIBRATION PROCEDURE FOR DISTANCE ATTENUATION

Input parameters required to perform broadband simulations using the hybrid procedure of Graves and Pitarka [2010] include those for the kinematic rupture model (fault dimensions, slip distribution, rise time, rupture velocity, etc.), additional parameters for the high-frequency source spectrum [c_0 (used for corner frequency), stress parameter σ_p, sub-fault dimension *dl*], and those related to analysis of Green's functions (crustal velocity profile, *Q* model, and number of ray paths).

All of these parameters are potential candidates for model calibration. In our current study, we choose to focus on the number of ray paths (i.e., geometric spreading) and the *Q* model to address the too-fast distance attenuation problem. The original ShakeOut simulations used only two rays for the high-frequency modeling: direct and Moho-reflected [Graves et al. 2011]. Within about 100 km of the fault, these two rays are dominant; however, at further distances, additional ray paths including multiple surface and Moho-reflected phases, as well as other super-critically crustal reflected phases, can become important. At large source-to-site distances, many rays may need to be considered to obtain the full response, although the dominant high-frequency phases are surface and Moho-reflected rays (e.g., Ou and Herrmann [1990]). For our calibration experiments, we utilized a total of four rays. In addition to the direct and Moho-reflected rays, we also considered: (1) a ray initially traveling upward from the source, reflecting at the surface and traveling down to the Moho, then reflecting back to the site; and (2) another ray initially traveling down from the source to the Moho, reflecting back up to the surface, reflecting back down to the Moho, then reflecting back to the site. Sensitivity tests using combinations up to a total of 10 rays indicated that the distance attenuation between 100 to 200 km was not strongly affected when more than four rays were used.

We used the crustal velocity profile of Boore and Joyner [1997], which has a V_{s30} of 1100 m/sec (Figure 2.2). This site condition was selected so that the simulations are consistent with the hard rock site condition of the NGA GMPEs, effectively removing nonlinear site amplification effects from the analysis. Source-related parameters will shift up or down the Fourier amplitude spectrum or portions thereof, but will generally not significantly affect the variation of ground motion with distance. We adjusted Q through parameter a (Equation 2.3), which was $a = 25$ in the reference broadband simulations. Through trial and error, we found that $a = 57$ with four rays effectively removes distance attenuation bias, which we demonstrate below. Increasing Q in this manner decreases material damping in the crust, hence decreasing the attenuation of ground motion. The effect of the increased number of ray paths was modest by comparison.

The effects of the modifications are demonstrated in Figure 4.1(a), where simulated spectral accelerations for the M_w 7.25 event are shown for the original (low) and proposed (high) Q. The Q increase raises spectral accelerations noticeably for rupture distance $R_{rup} > 50$ km. Figure 4.1(b) shows spectral acceleration residuals calculated using Equation (3.1), which fluctuate with R_{rup} but increase markedly at high Q for $R_{rup} > 50$ km.

The simulation results can be more easily visualized using median residuals [$\overline{R}_k(T)$ per Equation (3.2)], as shown in Figure 4.2. The figure shows median residuals for all four GMPEs using the proposed (high) Q and one reference set of residuals (using BA) for low Q. Note that the AS and CB residuals have a relatively strong negative trend at large distance because the GMPE slope (in log-log space) is effectively constant with respect to distance beyond the near-fault region, whereas the data falls off relatively rapidly for $R_{rup} > \sim50$ km as a result of the Q effect (shown in Figure 4.2 as a downward slope in the residuals). The BA and CY GMPEs have a distance-dependent slope that better accommodates this trend in the ground motions.

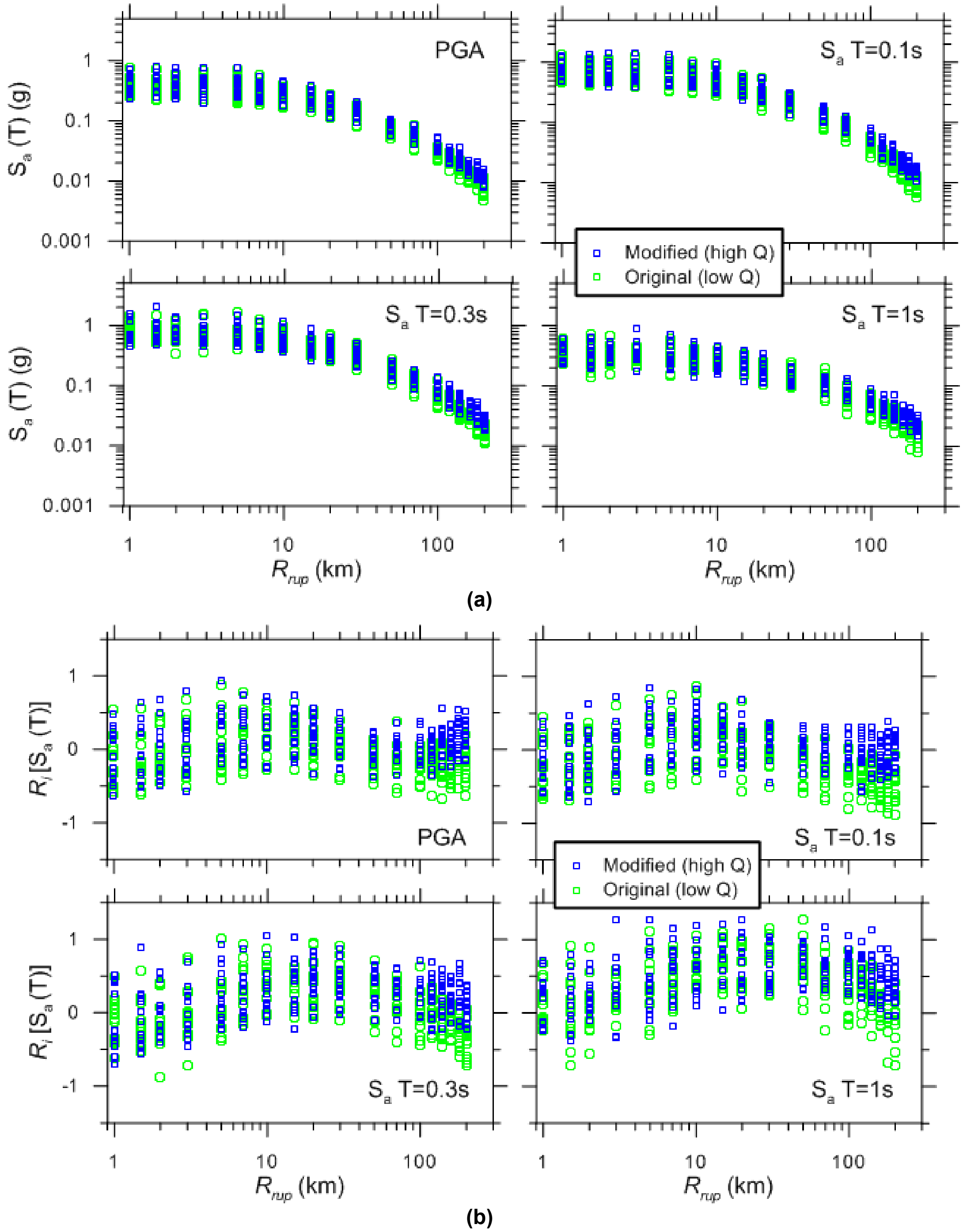

Figure 4.1 **(a) Spectral accelerations for original (low *Q*, 2 rays) and modified (high *Q*, 4 rays) high-frequency simulations of M_w 7.25 strike-slip earthquake; and (b) spectral acceleration residuals from simulated motions from (a) relative to BA GMPE.**

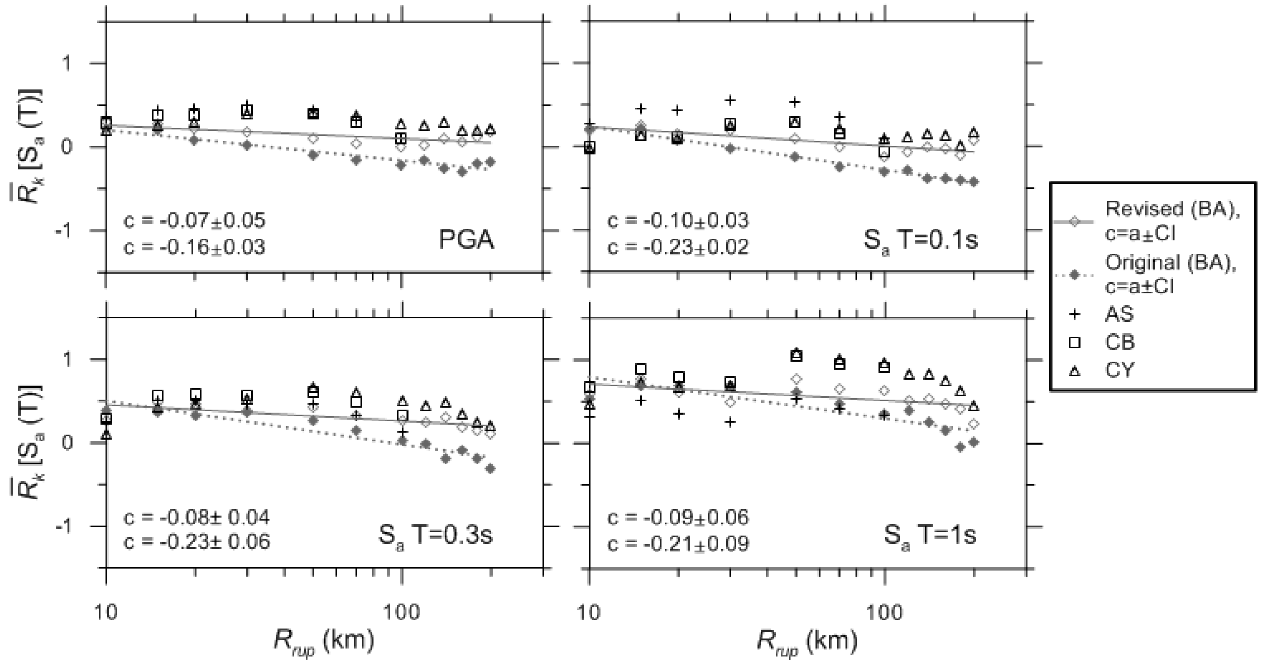

Figure 4.2 **Median residuals for modified (high *Q*, 4 rays) high-frequency simulations of M_w7.25 strike-slip earthquake (AS, BA, CB, CY GMPEs). Also shown are results for original (low *Q*, 2 rays) high-frequency simulation procedure (BA GMPE only). Fit lines with slope *c* are shown for BA; the slope is within its confidence interval (denoted CI in legend) and hence is not significantly different from zero for the modified simulations. The slope is significant for the original simulation procedure.**

The extent to which the data demonstrate distance-attenuation bias can be represented by the slope of the median residuals. Denoted as *c*, this slope is established by least-squares linear regression, as illustrated for BA in Figure 4.2. The fit is taken from 10–200 km distance for BA and CY but only from 10–100 km for AS and CB because of their restrictive distance attenuation function described above. Figure 4.3 shows slopes averaged across the four GMPEs as a function of period for the original and proposed *Q* values. The slopes are markedly negative for the original *Q*, slightly negative for the modified *Q* for M_w 5.0 and 6.5, and near zero for the modified *Q* for M_w 7.25 and 8. We judge this lack of trend for the larger simulated magnitudes to indicate the level of *Q* modification is adequate. Further increases of *Q* could have removed the bias at lower magnitudes, but at the expense of too-slow distance attenuation for large magnitude. Since the value of simulations is principally at larger magnitudes where recordings are sparse we choose to optimize the fit for those larger magnitudes.

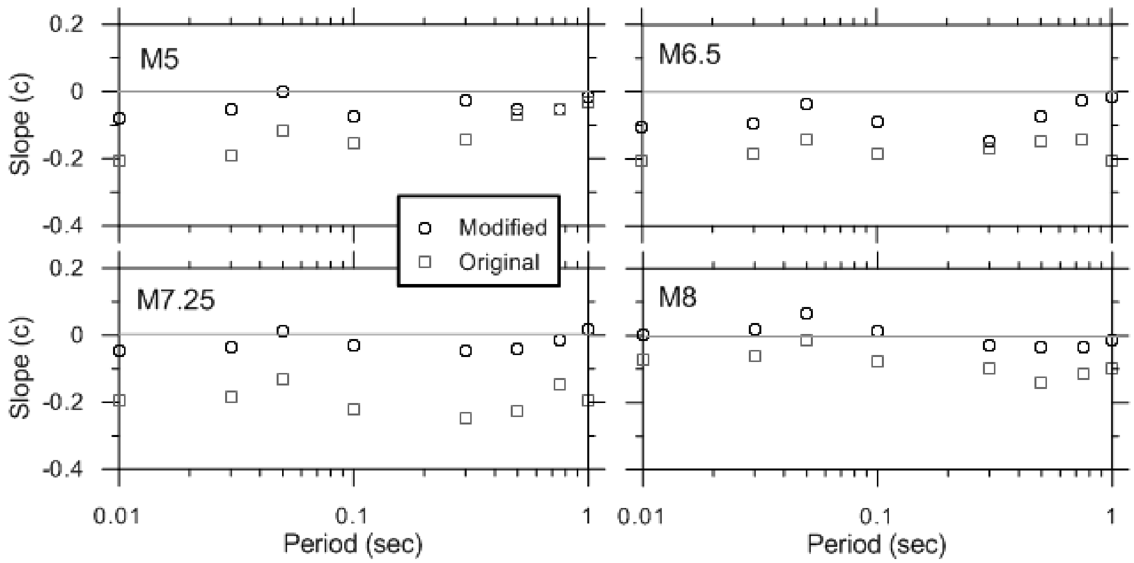

Figure 4.3 Slope parameter *c* (non-zero slope indicates misfit from GMPE) as function of spectral period for original (low *Q*, 2 rays) simulations and proposed modification (high *Q*, 4 rays). Values plotted are the averages across the four GMPE using 10–200 km for BA and CY and 10–100 km for AS and CB.

We checked our results for Q modification using the Northridge rock crustal velocity profile shown in Figure 2.2, which has V_{s30} = 865 m/sec (compare to V_{s30} = 1100 m/sec in the generic rock profile). The changed crustal velocities affect the ground motions but do not appreciably change distance attenuation trends (or their sensitivity to Q).

4.2 CALIBRATION PROCEDURE FOR INTRA-EVENT DISPERSION

To address the too-low intra-event dispersion, we began by randomizing crustal velocities relative to the Boore and Joyner [1997] model, which also affects Q values through Equation (1.2). This increases the dispersion of simulated motions, but only modestly. Since the Fourier phase at high frequencies in the simulation procedure are already fully random and randomization of path-related parameters (which affect Fourier amplitude) does not introduce significant dispersion, the only remaining option is to randomize source parameters (which also affect Fourier amplitude). Rather than randomize particular parameters in the source function, which were arbitrarily selected in the original model implementation, we simply randomize Fourier amplitudes directly. The randomization takes the Fourier amplitude from Equation (4.1) (after conversion to natural log units) as a median of a normal distribution [denoted A(f)].

Modifications are calculated as:

$$A_r(f) = A(f)\exp(\varepsilon\sigma_A) \tag{4.1}$$

where $A_r(f)$ denotes the randomized Fourier amplitude, σ_A is a frequency-independent log-normal standard deviation optimized in the present work, and ε is selected using a random number generator that produces realizations according to the standard normal distribution (mean of zero, standard deviation of one). This randomization assumes perfect correlation between frequencies and no correlation between simulations at different locations. We recognize that this is not strictly correct. Fourier amplitudes for a single site at neighboring frequencies exhibit only modest correlation [Ancheta et al. 2011], not the perfect correlation assumed here. For site locations separated by tens to hundreds of meters, spatial correlations are practically negligible [Ancheta et al.2011], which is consistent with the lack of correlation taken here.

Figure 4.4 shows intra-event dispersion for rock site conditions (V_{s30} = 1100 m/sec) from the NGA GMPEs as a function of period along with the dispersion from the non-randomized and randomized simulation procedures. All simulations utilized fault slip randomness and spatial correlation as described in Graves and Pitarka [2010] along with the modified path parameters described above (high Q, 4 ray paths). The non-randomized simulations produce dispersions significantly lower than those from GMPEs, except at M_w 8. The dispersion matches shown in Figure 4.4 were achieved with a Fourier amplitude randomization of σ_A = 0.45 (natural log units) for the M_w 5.0 and 6.5 simulations, σ_A = 0.35 for the M_w 7.25 simulation, and σ_A = 0 (no randomization) for the M_w 8 simulations. The reason for the magnitude-dependent σ_A is that slip randomization significantly affects ground motion dispersion when the fault dimensions are comparable or larger than the array dimensions. To reinforce this point, simulations were performed for the M_w 8 event using a smoothed slip model (derived by scaling the standard deviation of slip variations by a factor of 0.65, which is comparable to that used in ShakeOut); as shown in Figure 4.4, the intra-event dispersion from those simulations is markedly reduced.

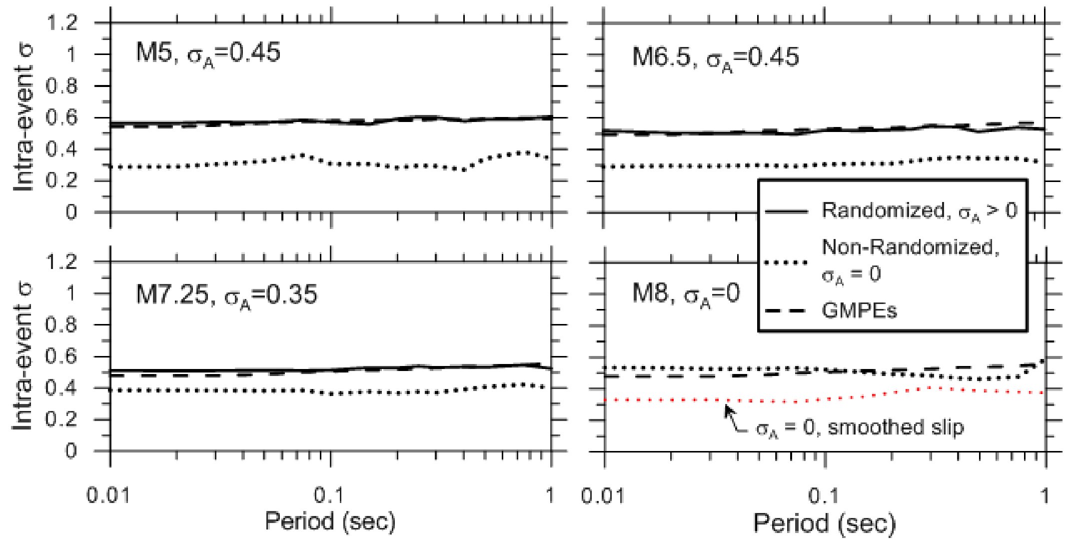

Figure 4.4 **Intra-event standard deviation σ for original (low *Q*, 2 rays) simulations and proposed modification (high *Q*, 4 rays) with magnitude-dependent randomization. All standard deviation terms plotted are the averages across the four NGA GMPEs.**

The variation of dispersion with distance is shown in Figure 4.5 for the M_w 6.5, 7.25, and 8 simulations. Results are shown with and without Fourier amplitude randomization. Simulations without randomization ($\sigma_A = 0$) show a dispersion decay with distance, whereas the introduction of Fourier amplitude randomization markedly reduces the distance trend. We interpret these trends as indicating that (1) randomization of the fault slip function introduces high dispersion near the fault but modest dispersion in the far field that is significantly below empirical dispersion estimates; and (2) randomization of Fourier amplitudes modestly affects near fault dispersion but significantly affects far-field dispersion. For the M_w 6.5 and 7.25 simulations, the overall dispersion levels with the proposed Fourier amplitude randomization are compatible with empirical estimates across the distance range considered. For the M_w 8 simulations, the near-source dispersion levels match empirical estimates without Fourier amplitude randomization but fall below empirical estimates at farther distances. We have chosen to not randomize these simulations, achieving a satisfactory near-field dispersion, but sacrificing to some extent the far-field dispersion levels.

(a)

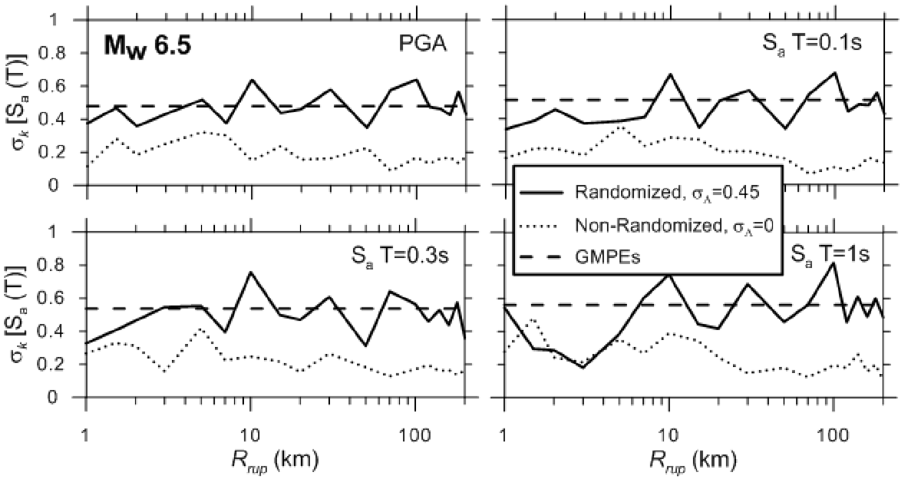

(b)

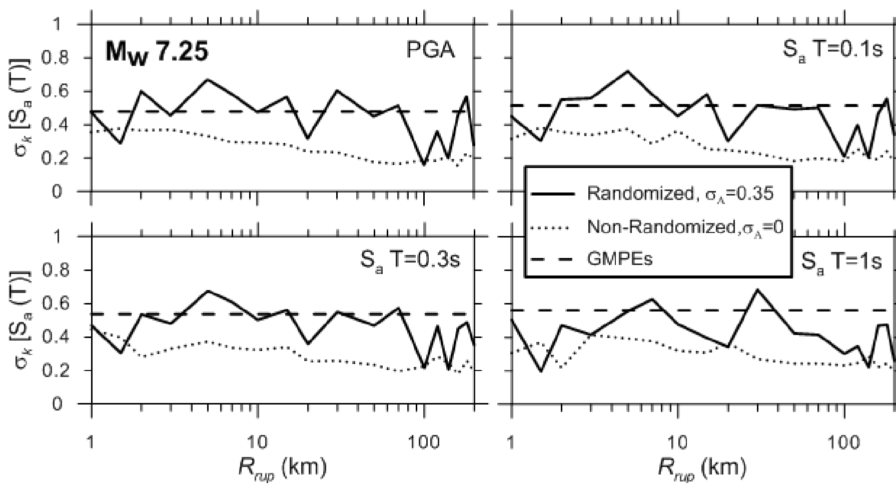

(c)

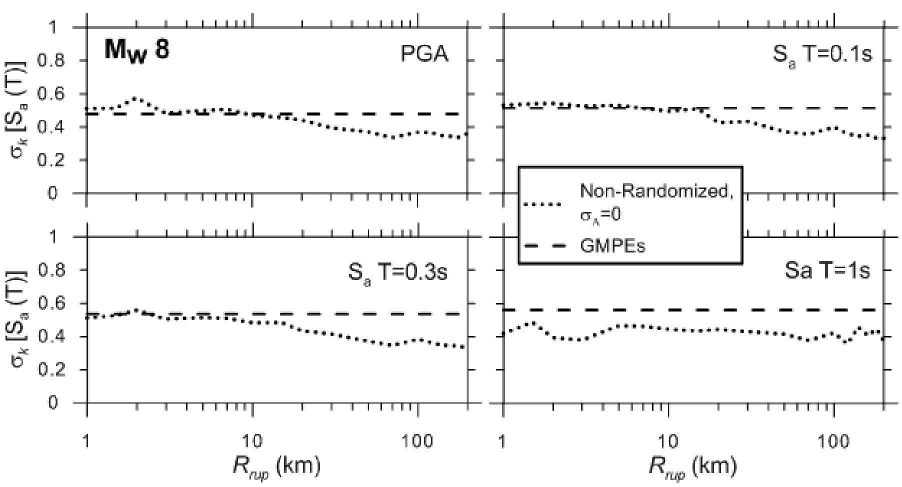

Figure 4.5 Variation with distance of intra-event standard deviation of modified simulations (high Q, 4 rays) relative to BA GMPE before and after randomization of Fourier amplitudes for (a) M_w 6.5, (b) M_w 7.25 and (c) M_w 8 strike slip earthquake. Intra event standard deviation terms plotted for GMPEs are the averages across the four NGA GMPEs.

5 Verification of Performance in Broadband Simulations

The calibration process described in previous sections operated on the high-frequency component of the simulation procedure. Here we verify that the modified high-frequency procedure produces satisfactory results when implemented in the full hybrid broadband methodology. This is done using broadband simulations of the ShakeOut event. The ShakeOut simulations were repeated using a revised source model reflecting the more heterogeneous slip distribution produced by the Graves and Pitarka [2010] method as well as the increased Q and the use of four ray paths instead of two. Because the magnitude is near 8, the Fourier amplitudes were not randomized ($\sigma_A = 0$). Those simulations are described further in Section 5.1. Section 5.2 presents the residuals analysis for the revised simulations.

5.1 REVISED SHAKEOUT SIMULATIONS

The original ShakeOut simulations used a kinematic rupture description based on a slip predictable model. This approach assumed that all accumulated strain since the most recent earthquake is released during the subsequent rupture. For the southern San Andreas fault considered in ShakeOut, the accumulated strain is estimated to be about 6 to 7 m along the Coachella segment, and about 3 to 4 m along the San Bernardino and Mojave segments. In the construction of the original ShakeOut scenario rupture, the long wavelength features (longer than about 30 km) were constrained to match these slip-predictable values. Shorter wavelength features were added using a randomized procedure. The resulting slip distribution is rather smooth, and in particular does not have many regions of low slip (which are typically observed in large surface rupturing earthquakes).

Here we have constructed an updated rupture characterization for the ShakeOut scenario using the method of Graves and Pitarka [2010]. The main differences between the updated scenario and the original scenario are as follows:

- Long wavelength slip distribution is not constrained by the slip-predictable model, asperity distribution is random with a wave number-squared falloff and standard error of slip set to 85% of mean slip. Mean slip and total seismic moment are the same as original rupture description. Resulting slip distribution has a more complex spatial distribution.
- Mean rupture speed is set at 85% of local shear wave velocity and scales with level of local slip (like original ShakeOut). However, scaling is not as strong so rupture tends to remain mostly sub-shear, whereas original ShakeOut had greater regions of super-shear rupture. Also, updated characterization has stronger short wavelength perturbations of rupture speed.
- The updated model uses a slightly different fault geometry composed of seven piecewise continuous rectangular fault segments. Fault surface in the original model is composed of triangulated elements, which are designed to more closely match the details of the actual fault. The differences in geometry should not have a significant impact on the simulated ground motions.

Figure 5.1 compares the surface projections of the original and updated fault representations. The seven segments of the updated model closely match the surface trace of the original representation. Most of the fault has a near vertical dip, except for the region along the San Gorgonio Pass where the fault dips towards the northeast. In the updated model, this section is approximated using two dipping segments.

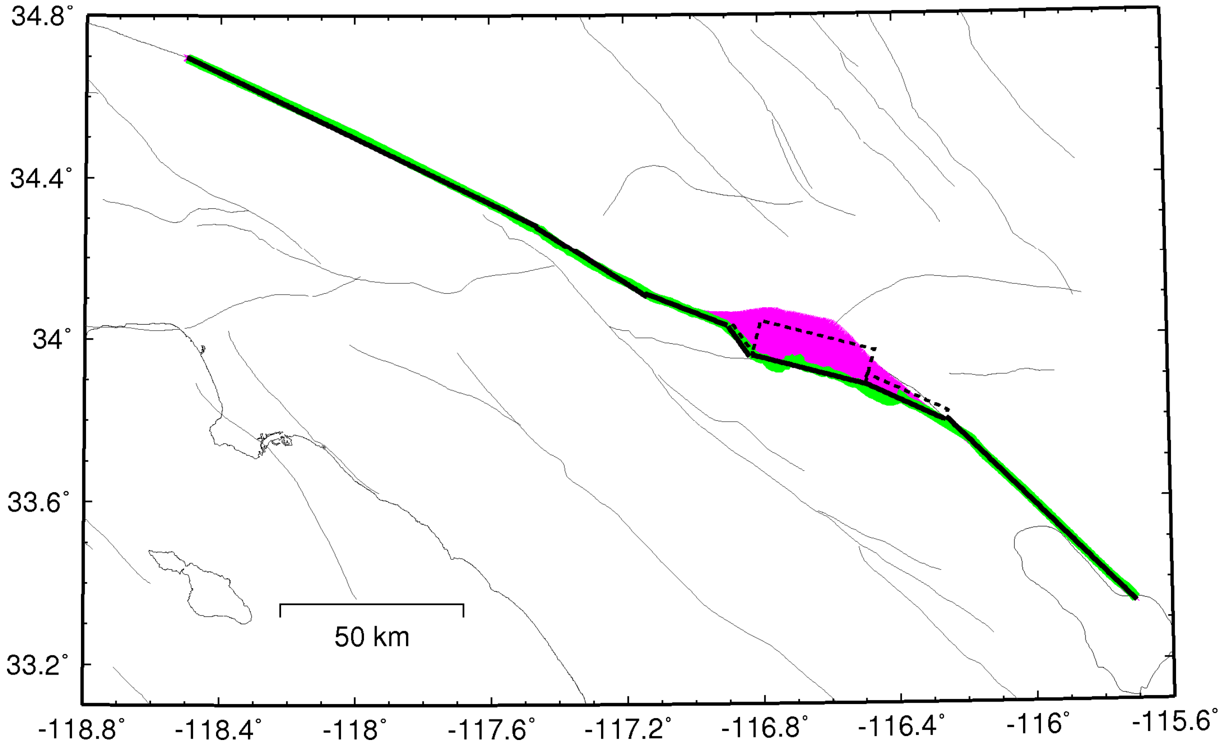

Figure 5.1 **Comparison of surface projection of ShakeOut fault geometry for original and updated models. The green line is surface trace of original model, and the magenta region indicates surface projection of dipping portion of original fault (dips to the northeast). The solid black line is surface trace of updated seven-segment fault model. The dashed portions indicate surface projection of dipping regions for updated fault model.**

Figure 5.2 compares the slip distribution and rupture front contours of the original and updated models. A large number of random realizations were initially generated for the updated model, and then a slip distribution was selected that was roughly similar to the original model (mainly the large slip along the southernmost section of the fault). The down-dip width of the updated model is constant at 15 km, whereas the original model varies from about 12 km to about 20 km (average is 15 km). Since both models extend to the ground surface, the differences in down-dip width should not significantly affect the radiated ground motions.

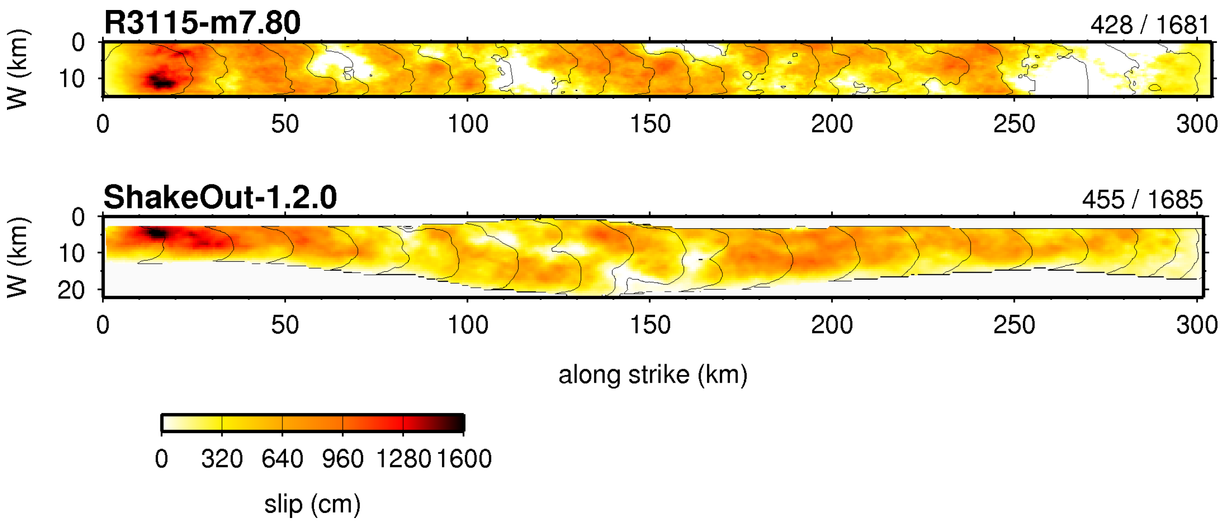

Figure 5.2 **Comparison of slip distribution and rupture propagation contours for original and updated ShakeOut models. The top panel is updated model, which has a fixed down-dip width of 15 km. The bottom panel is original model, which has a variable down-dip width. Both models rupture to the ground surface. The updated model exhibits stronger heterogeneity in both slip and rupture propagation.**

While the general pattern of slip distribution is roughly similar for the two models, there are notable differences. The main difference is the stronger heterogeneity of the updated model with tighter concentrations of large slip (asperities) and also the existence of regions of little or no slip. These features are not strongly present in the original model. The total seismic moment is constrained to be the same for both models (M_w 7.8) with the slight difference in mean slip (428 cm for the updated model versus 455 cm for the original) resulting from the differences in the depth distribution of the slip coupled with the generally increasing rigidity as a function of depth. Both models have similar peak slip amounts (1681 cm versus 1685 cm).

The other main difference between the two models is the coherency of the rupture propagation across the fault surface, as exhibited by the rupture front contours in Figure 5.2. The original model is characterized by fairly smooth rupture propagation with some longer wavelength perturbations occurring where the rupture speed correlates with the local slip values. The parameterization used in the updated model has a stronger correlation of rupture speed perturbations with the local slip, which leads to greater incoherence in the rupture front, particularly at shorter length scales.

Using the updated rupture model, we have performed two sets of broadband simulations. These simulations use the same parameterizations used for the original ShakeOut calculations.

For the low-frequency ($f < 1$ Hz) calculation, the updated rupture model is inserted into the same three-dimensional seismic velocity model used for the original calculations. For the high-frequency calculation, we first used the updated rupture model with the same parameterization as the original ShakeOut simulation (same one-dimensional seismic velocity and Q model, number of rays). Then, we ran a second high-frequency case, using the high Q model with 4 rays, as described in Chapter 4. The combination of the high-frequency and low-frequency responses into the broadband response was done in the same manner as the original ShakeOut calculation. Finally, we calculated and tabulated peak ground motion values and spectral accelerations (PGA, PGV, and S_a) for both of these updated simulations.

Figures 5.3 and 5.4 show peak ground motion maps (PGA, PGV, S_a at 0.3, 1, and 3 sec) for the original and updated ShakeOut simulations. These results are analyzed next.

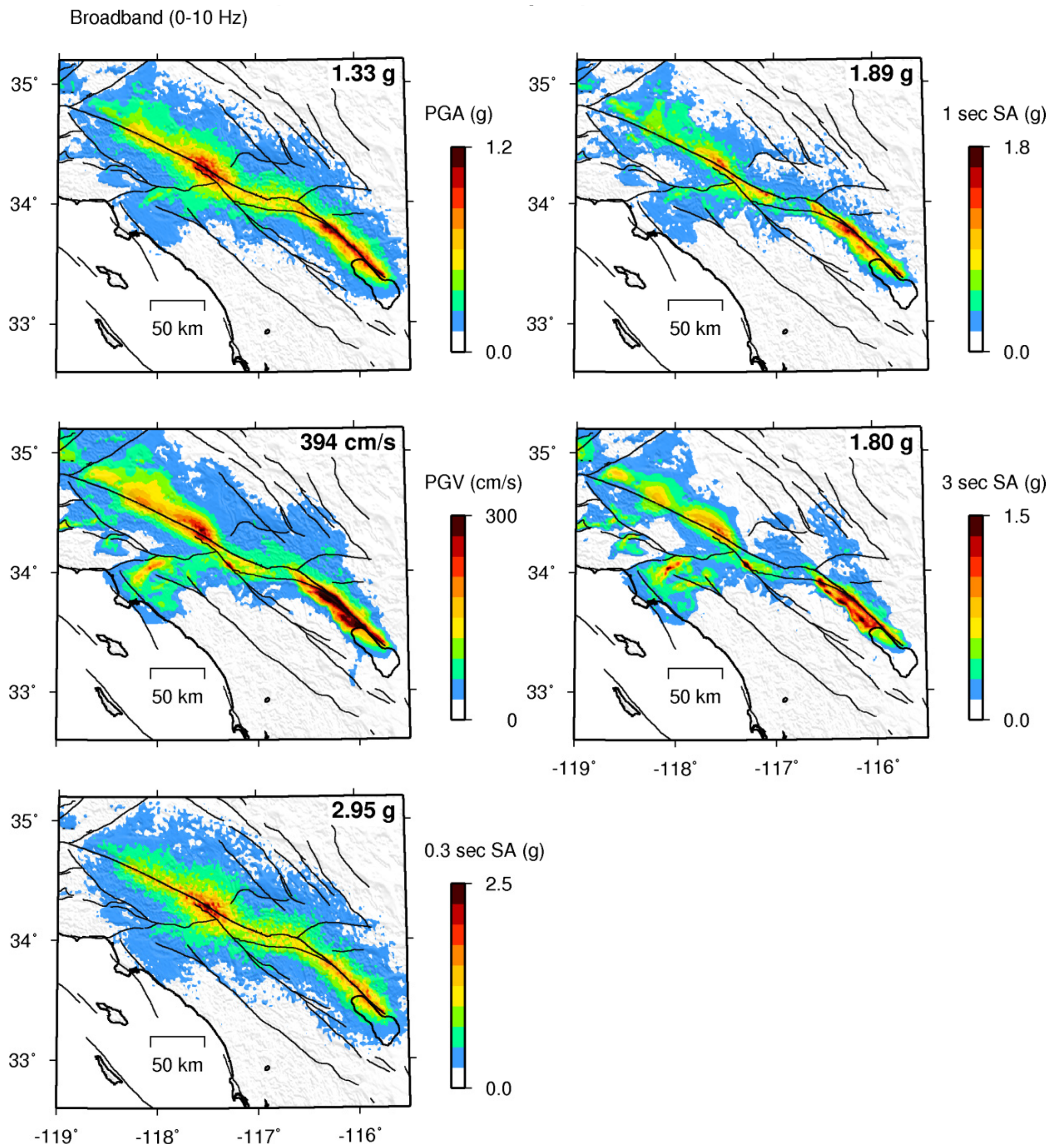

Figure 5.3 Maps of simulated ground motion values for original ShakeOut rupture. High-frequency simulation uses high *Q* model and 4 rays.

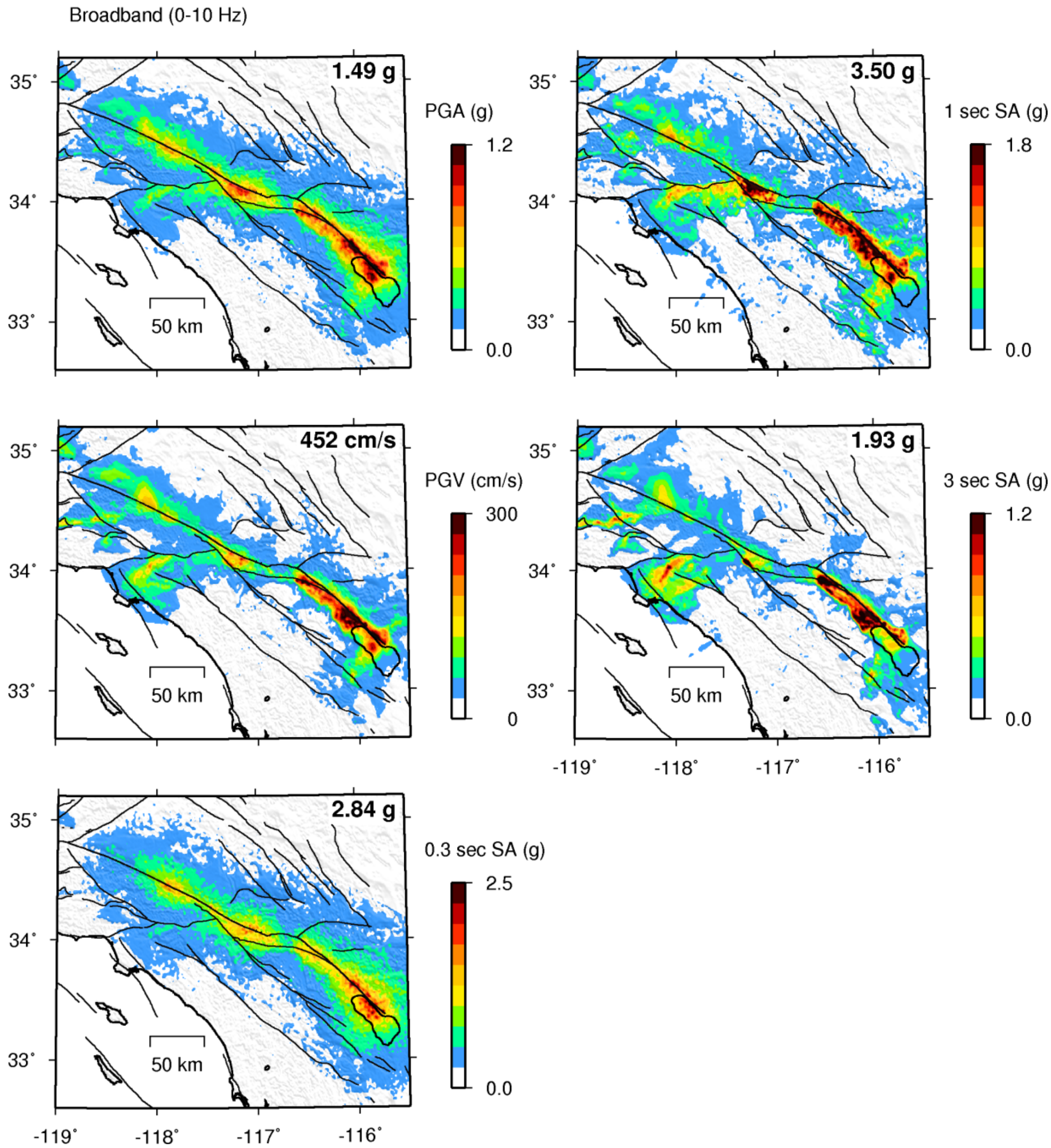

Figure 5.4 Maps of simulated ground motion values for updated ShakeOut rupture. High-frequency simulation uses high *Q* model and 4 rays.

5.2 RESIDUALS ANALYSIS USING REVISED SIMULATIONS

Residuals for both the original and updated ShakeOut simulations were calculated relative to the NGA GMPEs using Equation (3.1) and median residuals $\overline{R}_k(T)$ were calculated within distance bins using Equation (3.2). In Figure 5.5, those median residuals were plotted versus R_{rup} for the various IMs considered previously. The distance attenuation bias from the original ShakeOut simulations was significantly reduced for the BA and CY GMPEs. Substantial misfit remains (not shown in Figure 5.5) for AS and CB as a result of the distance attenuation function as described earlier (i.e., Figure 4.2). At a distance of 100 km, the difference between the original and updated median residuals for BA and CY is an increase of approximately 0.65 (in ln units), which nearly doubles predicted ground motions at this distance.

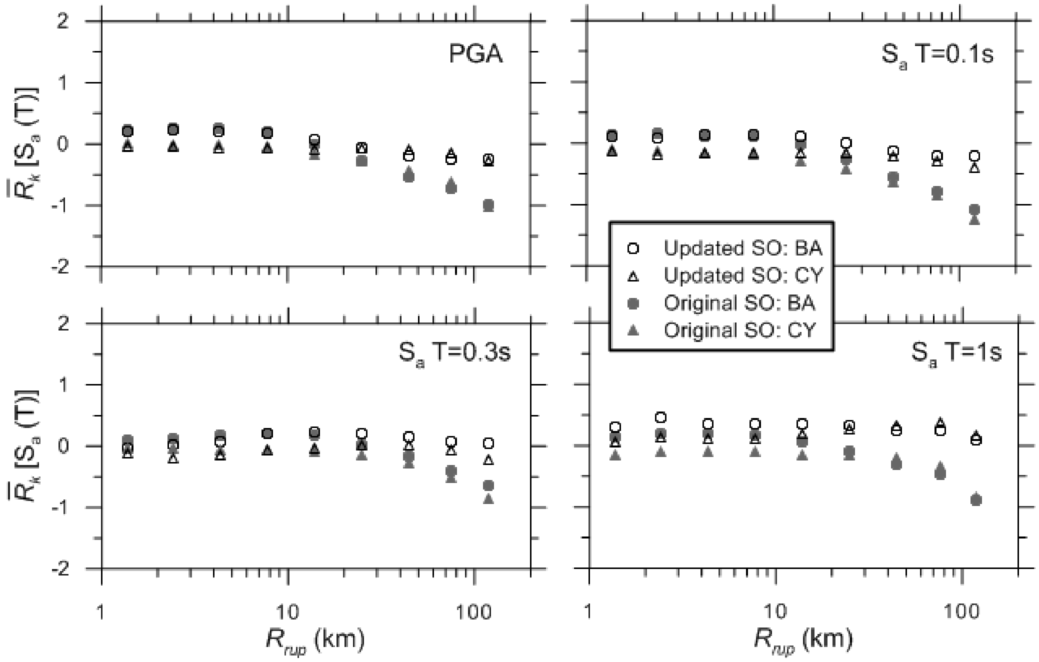

Figure 5.5 Median residuals relative to BA and CY GMPEs within distance bins for updated and original (a) ShakeOut simulations and (b) intra-event standard deviation of original and updated ShakeOut simulations compared to GMPEs.

Using the same distance bins as above for median residuals, standard deviations of intra-bin residuals were calculated in a manner that separates distance attenuation bias from the dispersion calculation, as follows:

$$Var(R) = \frac{\sum_{i=1}^{N_k}\left(R_i - \overline{R}_k\right)^2}{N_k - 1}$$

$$\sigma = \sqrt{Var(R)} \tag{5.1}$$

where N_k is the number of simulated motions in distance bin k. By subtracting distance-bin medians $\overline{R}_k$ in the variance calculation, bias in the distance attenuation is not mapped into the dispersion calculation. Figure 5.6 shows intra-event dispersions as a function of distance from original and updated ShakeOut simulations for various IMs. To reduce the effects of differences in site amplification modeling being mapped into the dispersion estimates, for this comparison we restricted our analysis to sites having $V_{s30} \geq 760$ m/sec. These results show a general decay of dispersion with distance, particularly for the shorter period metrics in the original simulation. The decays are similar to the high-frequency simulation dispersions in Figure 4.5. As described previously, we expected higher near-field dispersion in our simulations since this is primarily controlled by source heterogeneity in our approach. Because the level of source heterogeneity was increased for the updated ShakeOut simulations, the dispersions also increased for most spectral periods.

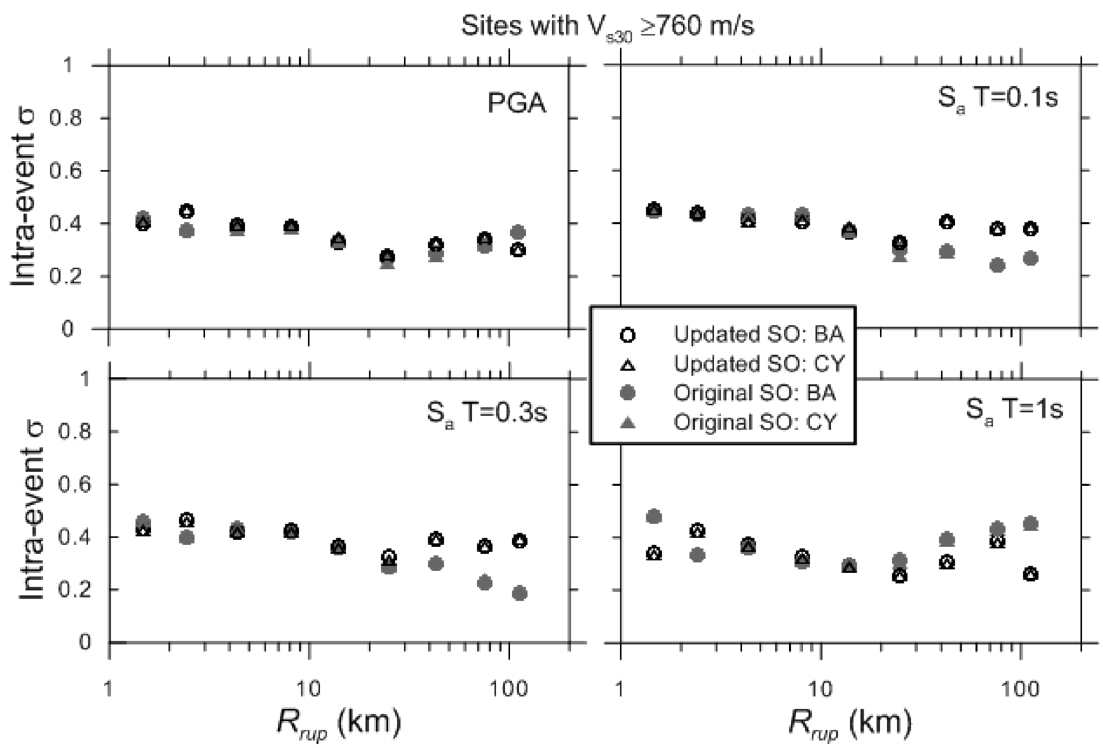

Figure 5.6 Variation with distance of intra-event standard deviations for the various IMs relative to BA and CY GMPEs for updated and original ShakeOut simulations. Sites are restricted to those with $V_{s30} \geq 760$ m/sec.

To facilitate comparisons to GMPE intra-event dispersions, we evaluated period-dependent intra-event dispersions that represent average values for near-field ($R_{rup} < 10$ km) and far-field ($R_{rup} > 100$ km) conditions. These dispersions were calculated as:

$$Var(R) = \frac{\sum_{k=1}^{N_{bins}} \sum_{i=1}^{N_k} \left(R_i - \overline{R}_k\right)^2}{\sum_{k=1}^{N_{bins}} N_k - N_{bins}}$$

$$\sigma = \sqrt{Var(R)} \tag{5.2}$$

where N_{bins} is the number of distance bins within the respective distance ranges (four for R_{rup} < 10 km; one for R_{rup} > 100 km). The subtraction of N_{bins} in the denominator reflects that number of degrees of freedom in the variance calculation. Figure 5.7 presents results of the above calculation, in which σ terms are computed using Equation (5.2) for all four NGA GMPEs and then averaged. The average intra-event standard deviation terms from the GMPEs are also shown. At close distances, the updated ShakeOut dispersions are generally consistent with GMPEs, falling somewhat low only between 0.1 and 1.0 sec. At long distances, a more consistent misfit remains between dispersion from GMPEs and the ShakeOut simulations, which is expected due to the lack of Fourier amplitude randomization for this magnitude, as described previously in Section 4.2. Figure 5.8 shows dispersion levels that occur if Fourier amplitude randomization is added in the manner described in Section 4.2 at the level of σ_A = 0.35. Near-fault dispersion is slightly over-estimated and far-field dispersion remains under-estimated. Hence, it does not appear that Fourier amplitude randomization alone can achieve dispersion levels compatible with GMPEs over a wide distance range.

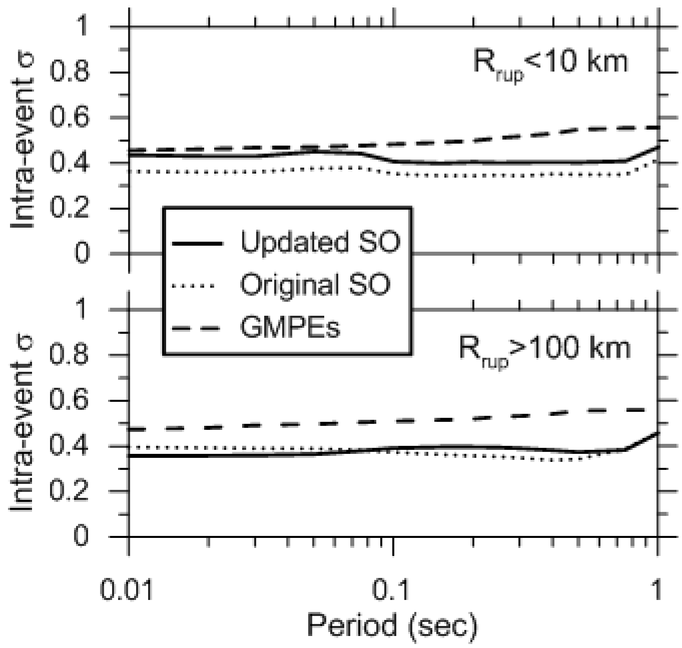

Figure 5.7 **Intra-event standard deviation for the updated and original ShakeOut simulations for near- and far-field distance bins. All standard deviation terms plotted are the averages across the four NGA GMPEs. The updated ShakeOut simulations have no Fourier amplitude randomization.**

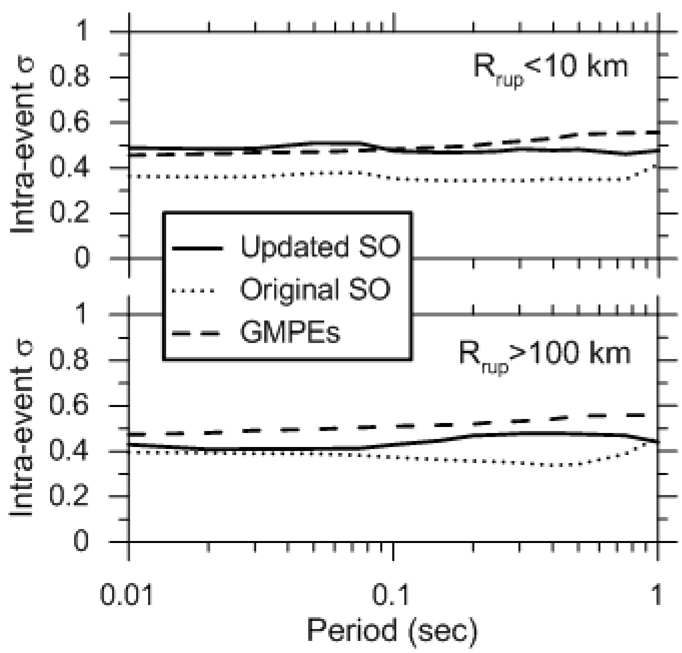

Figure 5.8 **This figure is identical to Figure 5.7, except the updated ShakeOut simulations now include Fourier amplitude randomization at the level of σ_A = 0.35.**

6 Conclusions

6.1 INTERPRETATIONS AND RECOMMENDATIONS

Broadband ground motion simulation procedures typically utilize physics-based modeling of source and path effects at low frequencies coupled with semi-stochastic procedures at high frequencies. Previous validation of the hybrid procedure of Graves and Pitarka [2010], which was used with some modification in the ShakeOut exercise and other earthquake scenario studies, demonstrated faster distance attenuation and lower dispersion of high-frequency ground motions than in empirical ground motion equations [Star et al. 2011].

As discussed by Star et al. [2011], when comparing attributes of simulated motions to GMPEs, one must consider whether a misfit indicates a problem with the simulations, the GMPEs, or both. The critical aspect is the degree to which the effect under consideration is well constrained in the empirical model. This is reflected to some extent by the consistency of GMPEs—which in turn relates to the sophistication of the GMPE functional forms (admittedly subjective)—but also to the amount of data available to constrain those portions of the empirical models. With regard to the distance attenuation discrepancy, attenuation of high-frequency IMs in the NGA models is well constrained up to approximately 100 km for magnitudes between approximately 5.5 and 7.5, and the various models are quite consistent [Abrahamson et al. 2008]. While the available data is sparse at the large magnitudes associated with the ShakeOut event, the potential for a large shift in distance attenuation rates from M_w 7.5 to 7.8 is low. Accordingly, we judge the deficiency in this case to lie mostly with the simulation. A similar rationale can be applied to the standard deviation terms. This motivates the work presented in this report, in which we seek to calibrate high-frequency components of the Graves and Pitarka [2010] simulation procedure to remove the too-fast distance attenuation and the too-low intra-event dispersion.

The high-frequency component of the simulation procedure combined a deterministic Fourier amplitude spectrum that is a function of closed-form source, path, and site models with a random phase. We increase crustal damping (*Q*) to reduce the distance attenuation bias. This is done by increasing parameter *a* in the frequency-independent portion of the *Q* model (Equation 2.2) from 25 to 57. Both the original and adjusted *Q* models are within the range provided by previous studies of *Q* using California earthquakes (Figure 2.2). We introduce random site-to-site variations to the Fourier amplitudes using a magnitude dependent log-normal standard deviation (0.45 for $M_w \leq 6.5$, 0.35 for M_w 7.25, and 0 for M_w 8). In general, this raises the intra-event standard deviations of response spectral accelerations to levels consistent with NGA GMPEs in terms of both their overall level and their variation with period. For the M_w 8 simulations, dispersions in the far field from the simulated motions fall below those from GMPEs, whereas dispersions are generally compatible in the near field.

The proposed changes to model parameters were implemented in a repeat of the broadband simulations for the ShakeOut event in which the increased source heterogeneity from Graves and Pitarka [2010], and the path modifications proposed herein (increased *Q*, additional ray paths) were implemented. The distance attenuation bias was found to be removed and intra-event dispersions were compatible with GMPEs at close distance. Dispersions were low in the far field; additional Fourier amplitude randomization for the large magnitudes would be necessary to improve this result.

6.2 RECOMMENDATIONS FOR FUTURE RESEARCH

Future research should consider several issues:

1. The calibration procedure (Chapter 4) should be expanded to address the following issues: (1) use a denser and more uniform set of sites; (2) consider additional magnitudes, particularly at the higher end (Mw 7.5, 7.75); (3) consider additional realizations for each magnitude (slip distribution and hypocenter; and (4) consider additional faulting styles.

2. Additional broadband simulation routines should be subject to the validation and calibration process described in Star et al. [2011] and in this report.

3. The validation process of the revised simulation procedure reported herein considered only a large magnitude event. Smaller magnitude validation events were not considered because none currently exist that include the updated protocols for source description (from Graves and Pitarka [2010]) and extend over a sufficiently large distance range to test the distance scaling function. Simulations meeting these criteria for smaller magnitude events of interest should be performed and validated.

4. Dispersion matches to the GMPE were achieved through a “brute force” process of Fourier amplitude randomization. It would be desirable to achieve addition dispersion through careful variations of physical parameters associated with the source and path models. For example, a more detailed and rigorous exploration of path-scattering effects would be warranted, especially in light of the observed distance dependence of dispersion in the current simulations.

5. Inter-event dispersion was not investigated in this work or other work that the authors are aware of. Validation of inter-event dispersion from simulation codes considering reasonable variations of source parameters is critical for engineering application of simulation procedures.

REFERENCES

Aagaard, B.T., T.M. Brocher, D. Dolenc, D. Dreger, R.W. Graves, S. Harmsen, S. Hartzell, S. Larsen, K. McCandless, S. Nilsson, N.A. Petersson, A. Rodgers, B. Sjögreen, and M.L. Zoback (2008). Ground-motion modeling of the 1906 San Francisco earthquake, Part II: Ground-motion estimates for the 1906 earthquake and scenario events, *Bull. Seismo. Soc. Am.*, 98:1012–1046.

Abrahamson, N.A., G.M. Atkinson, D.M. Boore, Y. Bozorgnia, K.W. Campbell, B.S-J. Chiou, I.M. Idriss, W.J. Silva, and R.R. Youngs (2008). Comparisons of the NGA ground-motion relations, *Earthq. Spectra*, 24:45–66.

Abrahamson, N.A., and W.J. Silva (2008). Summary of the Abrahamson and Silva NGA ground motion relations, *Earthq. Spectra*, 24:67–97.

Ameri, G., F Gallovič, F Pacor, and A Emolo (2009). Uncertainties in strong ground motion prediction with finite-fault synthetic seismograms: An application to the 1984 M5.7 Gubbio, central Italy, earthquake, *Bull. Seismo. Soc. Am.,* 99: 647–663.

Ancheta, T.D. (2010). Engineering characterization of spatially variable ground motions, *Ph.D. Dissertation*, Dept. of Civil and Environmental Engineering, University of California, Los Angeles.

Anderson, J.G., and S.E. Hough (1984). A model for the shape of the Fourier amplitude spectrum of acceleration at high frequencies, *Bull. Seismo. Soc. Am.*, 74:1969–1993.

Atkinson, G.M., K. Assatourians, D.M. Boore, K.W. Campbell, and D. Motazedian (2009). A guide to differences between stochastic point-source and stochastic finite-fault simulations, *Bull. Seismo. Soc. Am.,* 99: 3192–3201, doi: 10.1785/0120090058.

Beresnev, I.A., and G.M. Atkinson (1997). Modeling finite-fault radiation from the ωn spectrum, *Bull. Seismo. Soc. Am.*, 87:67–84.

Bielak, J., R.W. Graves, K.B. Olsen, R. Taborda, L. Ramirez-Guzman, S.M. Day, G.P. Ely, D. Roten, T.H. Jordan, P.J. Maechling, J. Urbanic, Y.F. Cui, G. Juve (2010). The ShakeOut earthquake scenario: Verification of three simulation sets, *Geophy. J. International*, 180:375–404.

Boore, D.M. (1983). Stochastic simulation of high-frequency ground motions based on seismological models of the radiated spectra, *Bull. Seismo. Soc. Am.,* 73:1865–1894.

Boore, D.M., and W.B. Joyner (1997). Site amplifications for generic rock sites, *Bull. Seismo. Soc. Am.*, 87:327–341.

Boore, D.M., and G.M. Atkinson (2008). Ground motion prediction equations for the average horizontal component of PGA, PGV, and 5%-damped PSA at spectral periods between 0.01 and 10.0 s, *Earthq. Spectra*, 24:99–138.

Campbell, K.W., and Y. Bozorgnia (2008). NGA ground motion model for the geometric mean horizontal component of PGA, PGV, PGD and 5% damped linear elastic response spectra for periods ranging from 0.01 to 10s, *Earthq. Spectra*, 24:139–172.

Campbell, K.W. (2009). Estimates of shear-wave Q and κ0 for unconsolidated and semiconsolidated sediments in eastern North America, *Bull. Seismo. Soc. Am.*, 99:2365–2392.

Chiou, B.S-J., R. Darragh, D. Dreger, and W.J. Silva (2008). NGA project strong-motion database, *Earthq. Spectra*, 24:23-44.

Chiou, B.S-J., and R.R. Youngs (2008). Chiou and Youngs PEER-NGA empirical ground motion model for the average horizontal component of peak acceleration and pseudo-spectral acceleration for spectral periods of 0.01 to 10 seconds, *Earthq. Spectra*, 24:173-215.

Conte, J.P., and B.F. Peng (1997). Fully nonstationary analytical earthquake ground-motion model. *J. Engrg. Mech.*, 12:15–24.

Day, S.M., R.W. Graves, J. Bielak, D.S. Dreger, S. Larsen, K.B. Olsen, A. Pitarka, and L. Ramirez-Guzman (2008). Model for basin effects on long-period response spectra in Southern California, *Earthq. Spectra*, 24:257-277.

Fatehi, A., and R.B. Herrmann (2008). High-frequency ground-motion scaling in the Pacific northwest and in northern and central California, *Bull. Seismo. Soc. Am.*, 98:709–721.

Frankel, A. (1993). Three-dimensional simulations of ground motions in the San Bernardino Valley, California, for hypothetical earthquakes on the San Andreas fault, *Bull. Seismo. Soc. Am.*, 83:1020–1041.

Frankel, A. (1995). Simulating strong motions of large earthquakes using recordings of small earthquakes: The Loma Prieta mainshock as a test case, *Bull. Seismo. Soc. Am*. 85,:1144–1160.

Frankel, A. (2009). A constant stress-drop model for producing broadband synthetic seismograms: Comparison with the Next Generation Attenuation relations, *Bull. Seismo. Soc. Am.*, 99:664–680.

Graves, R.W., B.T. Aagaard, K.W. Hudnut, L.M. Star, J.P. Stewart, and T.H. Jordan (2008). Broadband simulations for M_w 7.8 southern San Andreas earthquakes: Ground motion sensitivity to rupture speed, *Geophys. Res. Lett.,* 35, L22302, doi:10.1029/2008GL035750.

Graves, R.W., and A. Pitarka (2010). Broadband ground-motion simulation using a hybrid approach, *Bull. Seismo. Soc. Am.*, 100:2095–2123.

Graves, R.W., B. T. Aagaard, and K.W. Hudnut (2011). The ShakeOut earthquake source and ground motion simulations, *Earthq. Spectra*, 27 (2):273–291.

Guatteri, M., P.M. Mai, and G.C. Beroza (2004). A pseudo-dynamic approximation to dynamic rupture models for strong ground motion prediction, *Bull. Seismo. Soc. Am.*, 94:2051–2063.

Harmsen, S., and A. Frankel (2001). Geographic deaggregation of seismic hazard in the United States, *Bull. Seismo. Soc. Am.*, 83:13–26.

Hartzell, S, S. Harmsen, A. Frankel, and S. Larsen (1999). Calculation of broadband time histories of ground motion: Comparison of methods and validation using strong-ground motion from the 1994 Northridge Earthquake, *Bull. Seismo. Soc. Am.,* 89:1484–1504.

Hartzell, S., M. Guatteri, P.M. Mai, P-C. Liu, and M. Fisk (2005). Calculation of broadband time histories of ground motion, Part II: Kinematic and dynamic modeling using theoretical Green's functions and comparison with the 1994 Northridge earthquake, *Bull. Seismo. Soc. Am.* 95:614–645

Liu, H., and D.V. Helmberger (1985). The 23:19 aftershock of the October 1979 Imperial Valley earthquake: More evidence for an asperity, *Bull. Seismo. Soc. Am.,* 75:689–708.

Liu, P., R.J. Archuleta, and S.H. Hartzell. (2006). Prediction of broadband ground-motion time histories: hybrid low/high- frequency method with correlated random source parameters, *Bull. Seismo. Soc. Am*., 96:2118–2130.

Mai, P.M., W. Imperatori, and K.B. Olsen (2010). Hybrid broadband ground-motion simulations: combining long-period deterministic synthetics with high-frequency multiple S-to-S backscattering, *Bull. Seismo. Soc. Am.*, 100, 2124–2142.

Mena, B., P.M. Mai, K.B. Olsen, M.D. Purvance, and J.N. Brune (2010). Hybrid broadband ground-motion simulation using scattering green's functions: application to large-magnitude events, *Bull. Seismo. Soc. Am*., 100:2143–2162.

Olsen, K.B., S.M. Day, J.B. Minster, Y. Cui, A. Chourasia, D. Okaya, P. Maechling, and T. Jordan (2008). TeraShake2: Simulation of Mw 7.7 earthquakes on the southern San Andreas with spontaneous rupture description, *Bull. Seismo. Soc. Am*., 98:1162–1185.

Olsen, K.B., S.M. Day, L.A. Dalguer, J. Mayhew, Y. Cui, J. Zhu, V.M. Cruz-Atienza, D. Roten, P. Maechling, T.H. Jordan, D. Okaya, and A. Chourasia (2009). ShakeOut-D: Ground motion estimates using an ensemble of large earthquakes on the southern San Andreas fault with spontaneous rupture propagation, *Geophy. Res. Lett.*, 36, L04303, doi:10.1029/2008GL036832.

Olsen, K.B., and J.E. Mayhew (2010). Goodness-of-fit criteria for broadband synthetic seismograms, with application to the 2008 Mw 5.4 Chino Hills, California, earthquake, *Seismo. Res. Lett*., 81:715–723.

Porter, K.A., L. Jones, D. Cox, J. Goltz, K. W. Hudnut, D. Mileti, S. Perry, D. Ponti, M. Reichle, C.R. Scawthorn, H.A. Seligson, K.I. Shoaf and A. Wein, (2011). The ShakeOut scenario: a hypothetical Mw7.8 earthquake on the southern San Andreas fault, *Earthq. Spectra,* 27, 2, 239–261.

Pulido, N., and L.A. Dalguer (2009). Estimation of the high-frequency radiation of the 2000 Tottori (Japan) earthquake based on a dynamic model of fault rupture: Application to the strong ground motion simulation, *Bull. Seismo. Soc. Am.*, 99:2305–2322.

Raoof, M., R.B. Herrmann, and L. Malagnini (1999). Attenuation and excitation of three-component ground motion in Southern California, *Bull. Seismo. Soc. Am.* 89:888–902.

Rezaeian, S., and A. Der Kiureghian (2008). A stochastic ground motion model with separable temporal and spectral nonstationarities, *Earthq. Engrg. Struct. Dyn.*, 37:1565–1584.

Sato, T., R.W. Graves, and P.G. Somerville (1999). Three-dimensional finite-difference simulations of long-period strong motions in the Tokyo metropolitan area during the 1990 Odawara earthquake (MJ 5.1) and the great 1923 Kanto earthquake (MS 8.2) in Japan, *Bull. Seismo. Soc. Am*., 89:579–607.

Sato, H. and M.C. Fehler (1998). *Seismic Wave Propagation and Scattering in the Heterogeneous Earth*, Springer-Verlag New York, Inc.

Schmedes, J., R.J. Archuleta, and D. Lavalle (2010). Correlation of earthquake source parameters inferred from dynamic rupture simulations, *J. Geophys. Res.* 115, doi 10.1029/2009JB006689.

Silva, W.J., and R.B. Darragh (1995). Engineering characterization of earthquake strong ground motion recorded at rock sites, *Report TR-102261*, Electric Power Research Institute, Palo Alto, CA.

Silva, W.J., S. Li, R. Darragh, and N. Gregor (1999). Surface geology based strong motion amplification factors for the San Francisco Bay and Los Angeles areas, Report to Pacific Earthquake Engineering Research Center.

Star, L. M., J.P. Stewart, and R.W. Graves (2011). Comparison of ground motions from hybrid simulations to NGA prediction equations, *Earthq. Spectra*, 27(2): 333–350.

Stidham, C., M. Antolik, D.S. Dreger, S. Larsen, and B. Ramanowicz (1999). Three-dimensional structure influences on the strong motion wavefield of the 1989 Loma Prieta earthquake, *Bull. Seismo. Soc. Am.*, 89:1184–1202.

Xu, J., J. Bielak, O. Ghattas, and J. Wang (2003). Three-dimensional nonlinear seismic ground motion modeling in basins, *Physics of the Earth and Planetary Interiors*, 137:81–95.

Zeng, Y., J.G. Anderson, and G. Yu (1994). A composite source model for computing realistic synthetics strong ground motions, *Geophy. Res. Lett.,* 21:725–728.

PEER REPORTS

PEER reports are available individually or by yearly subscription. PEER reports can be ordered at http://peer.berkeley.edu/publications/peer_reports.html or by contacting the Pacific Earthquake Engineering Research Center, 325 Davis Hall mail code 1792, Berkeley, CA 94720. Tel.: (510) 642-3437; Fax: (510) 665-1655; Email: peer_editor@berkeley.edu

PEER 2011/09 *Calibration of Semi-Stochastic Procedure for Simulating High-Frequency Ground Motions.* Jonathan P. Stewart, Emel Seyhan, and Robert W. Graves. December 2011.

PEER 2011/08 *Water Supply in regard to Fire Following Earthquake.* Charles Scawthorn. November 2011.

PEER 2011/07 *Seismic Risk Management in Urban Areas. Proceedings of a U.S.-Iran-Turkey Seismic Workshop.* September 2011.

PEER 2011/06 *The Use of Base Isolation Systems to Achieve Complex Seismic Performance Objectives.* Troy A. Morgan and Stephen A. Mahin. July 2011.

PEER 2011/05 *Case Studies of the Seismic Performance of Tall Buildings Designed by Alternative Means.* Task 12 Report for the Tall Buildings Initiative. Jack Moehle, Yousef Bozorgnia, Nirmal Jayaram, Pierson Jones, Mohsen Rahnama, Nilesh Shome, Zeynep Tuna, John Wallace, Tony Yang, and Farzin Zareian. July 2011.

PEER 2011/04 *Recommended Design Practice for Pile Foundations in Laterally Spreading Ground.* Scott A. Ashford, Ross W. Boulanger, and Scott J. Brandenberg. June 2011.

PEER 2011/03 *New Ground Motion Selection Procedures and Selected Motions for the PEER Transportation Research Program.* Jack W. Baker, Ting Lin, Shrey K. Shahi, and Nirmal Jayaram. March 2011.

PEER 2011/02 *A Bayesian Network Methodology for Infrastructure Seismic Risk Assessment and Decision Support.* Michelle T. Bensi, Armen Der Kiureghian, and Daniel Straub. March 2011.

PEER 2011/01 *Demand Fragility Surfaces for Bridges in Liquefied and Laterally Spreading Ground.* Scott J. Brandenberg, Jian Zhang, Pirooz Kashighandi, Yili Huo, and Minxing Zhao. March 2011.

PEER 2010/05 *Guidelines for Performance-Based Seismic Design of Tall Buildings.* Developed by the Tall Buildings Initiative. November 2010.

PEER 2010/04 *Application Guide for the Design of Flexible and Rigid Bus Connections between Substation Equipment Subjected to Earthquakes.* Jean-Bernard Dastous and Armen Der Kiureghian. September 2010.

PEER 2010/03 *Shear Wave Velocity as a Statistical Function of Standard Penetration Test Resistance and Vertical Effective Stress at Caltrans Bridge Sites.* Scott J. Brandenberg, Naresh Bellana, and Thomas Shantz. June 2010.

PEER 2010/02 *Stochastic Modeling and Simulation of Ground Motions for Performance-Based Earthquake Engineering.* Sanaz Rezaeian and Armen Der Kiureghian. June 2010.

PEER 2010/01 *Structural Response and Cost Characterization of Bridge Construction Using Seismic Performance Enhancement Strategies.* Ady Aviram, Božidar Stojadinović, Gustavo J. Parra-Montesinos, and Kevin R. Mackie. March 2010.

PEER 2009/03 *The Integration of Experimental and Simulation Data in the Study of Reinforced Concrete Bridge Systems Including Soil-Foundation-Structure Interaction.* Matthew Dryden and Gregory L. Fenves. November 2009.

PEER 2009/02 *Improving Earthquake Mitigation through Innovations and Applications in Seismic Science, Engineering, Communication, and Response. Proceedings of a U.S.-Iran Seismic Workshop.* October 2009.

PEER 2009/01 *Evaluation of Ground Motion Selection and Modification Methods: Predicting Median Interstory Drift Response of Buildings.* Curt B. Haselton, Ed. June 2009.

PEER 2008/10 *Technical Manual for Strata.* Albert R. Kottke and Ellen M. Rathje. February 2009.

PEER 2008/09 *NGA Model for Average Horizontal Component of Peak Ground Motion and Response Spectra.* Brian S.-J. Chiou and Robert R. Youngs. November 2008.

PEER 2008/08 *Toward Earthquake-Resistant Design of Concentrically Braced Steel Structures.* Patxi Uriz and Stephen A. Mahin. November 2008.

PEER 2008/07 *Using OpenSees for Performance-Based Evaluation of Bridges on Liquefiable Soils.* Stephen L. Kramer, Pedro Arduino, and HyungSuk Shin. November 2008.

PEER 2008/06 *Shaking Table Tests and Numerical Investigation of Self-Centering Reinforced Concrete Bridge Columns.* Hyung IL Jeong, Junichi Sakai, and Stephen A. Mahin. September 2008.

PEER 2008/05 *Performance-Based Earthquake Engineering Design Evaluation Procedure for Bridge Foundations Undergoing Liquefaction-Induced Lateral Ground Displacement.* Christian A. Ledezma and Jonathan D. Bray. August 2008.

PEER 2008/04 *Benchmarking of Nonlinear Geotechnical Ground Response Analysis Procedures.* Jonathan P. Stewart, Annie On-Lei Kwok, Yousseff M. A. Hashash, Neven Matasovic, Robert Pyke, Zhiliang Wang, and Zhaohui Yang. August 2008.

PEER 2008/03 *Guidelines for Nonlinear Analysis of Bridge Structures in California.* Ady Aviram, Kevin R. Mackie, and Božidar Stojadinović. August 2008.

PEER 2008/02 *Treatment of Uncertainties in Seismic-Risk Analysis of Transportation Systems.* Evangelos Stergiou and Anne S. Kiremidjian. July 2008.

PEER 2008/01 *Seismic Performance Objectives for Tall Buildings.* William T. Holmes, Charles Kircher, William Petak, and Nabih Youssef. August 2008.

PEER 2007/12 *An Assessment to Benchmark the Seismic Performance of a Code-Conforming Reinforced Concrete Moment-Frame Building.* Curt Haselton, Christine A. Goulet, Judith Mitrani-Reiser, James L. Beck, Gregory G. Deierlein, Keith A. Porter, Jonathan P. Stewart, and Ertugrul Taciroglu. August 2008.

PEER 2007/11 *Bar Buckling in Reinforced Concrete Bridge Columns.* Wayne A. Brown, Dawn E. Lehman, and John F. Stanton. February 2008.

PEER 2007/10 *Computational Modeling of Progressive Collapse in Reinforced Concrete Frame Structures.* Mohamed M. Talaat and Khalid M. Mosalam. May 2008.

PEER 2007/09 *Integrated Probabilistic Performance-Based Evaluation of Benchmark Reinforced Concrete Bridges.* Kevin R. Mackie, John-Michael Wong, and Božidar Stojadinović. January 2008.

PEER 2007/08 *Assessing Seismic Collapse Safety of Modern Reinforced Concrete Moment-Frame Buildings.* Curt B. Haselton and Gregory G. Deierlein. February 2008.

PEER 2007/07 *Performance Modeling Strategies for Modern Reinforced Concrete Bridge Columns.* Michael P. Berry and Marc O. Eberhard. April 2008.

PEER 2007/06 *Development of Improved Procedures for Seismic Design of Buried and Partially Buried Structures.* Linda Al Atik and Nicholas Sitar. June 2007.

PEER 2007/05 *Uncertainty and Correlation in Seismic Risk Assessment of Transportation Systems.* Renee G. Lee and Anne S. Kiremidjian. July 2007.

PEER 2007/04 *Numerical Models for Analysis and Performance-Based Design of Shallow Foundations Subjected to Seismic Loading.* Sivapalan Gajan, Tara C. Hutchinson, Bruce L. Kutter, Prishati Raychowdhury, José A. Ugalde, and Jonathan P. Stewart. May 2008.

PEER 2007/03 *Beam-Column Element Model Calibrated for Predicting Flexural Response Leading to Global Collapse of RC Frame Buildings.* Curt B. Haselton, Abbie B. Liel, Sarah Taylor Lange, and Gregory G. Deierlein. May 2008.

PEER 2007/02 *Campbell-Bozorgnia NGA Ground Motion Relations for the Geometric Mean Horizontal Component of Peak and Spectral Ground Motion Parameters.* Kenneth W. Campbell and Yousef Bozorgnia. May 2007.

PEER 2007/01 *Boore-Atkinson NGA Ground Motion Relations for the Geometric Mean Horizontal Component of Peak and Spectral Ground Motion Parameters.* David M. Boore and Gail M. Atkinson. May. May 2007.

PEER 2006/12 *Societal Implications of Performance-Based Earthquake Engineering.* Peter J. May. May 2007.

PEER 2006/11 *Probabilistic Seismic Demand Analysis Using Advanced Ground Motion Intensity Measures, Attenuation Relationships, and Near-Fault Effects.* Polsak Tothong and C. Allin Cornell. March 2007.

PEER 2006/10 *Application of the PEER PBEE Methodology to the I-880 Viaduct.* Sashi Kunnath. February 2007.

PEER 2006/09 *Quantifying Economic Losses from Travel Forgone Following a Large Metropolitan Earthquake.* James Moore, Sungbin Cho, Yue Yue Fan, and Stuart Werner. November 2006.

PEER 2006/08 *Vector-Valued Ground Motion Intensity Measures for Probabilistic Seismic Demand Analysis*. Jack W. Baker and C. Allin Cornell. October 2006.

PEER 2006/07 *Analytical Modeling of Reinforced Concrete Walls for Predicting Flexural and Coupled–Shear-Flexural Responses.* Kutay Orakcal, Leonardo M. Massone, and John W. Wallace. October 2006.

PEER 2006/06 *Nonlinear Analysis of a Soil-Drilled Pier System under Static and Dynamic Axial Loading.* Gang Wang and Nicholas Sitar. November 2006.

PEER 2006/05 *Advanced Seismic Assessment Guidelines.* Paolo Bazzurro, C. Allin Cornell, Charles Menun, Maziar Motahari, and Nicolas Luco. September 2006.

PEER 2006/04 *Probabilistic Seismic Evaluation of Reinforced Concrete Structural Components and Systems.* Tae Hyung Lee and Khalid M. Mosalam. August 2006.

PEER 2006/03 *Performance of Lifelines Subjected to Lateral Spreading.* Scott A. Ashford and Teerawut Juirnarongrit. July 2006.

PEER 2006/02 *Pacific Earthquake Engineering Research Center Highway Demonstration Project.* Anne Kiremidjian, James Moore, Yue Yue Fan, Nesrin Basoz, Ozgur Yazali, and Meredith Williams. April 2006.

PEER 2006/01 *Bracing Berkeley. A Guide to Seismic Safety on the UC Berkeley Campus.* Mary C. Comerio, Stephen Tobriner, and Ariane Fehrenkamp. January 2006.

PEER 2005/16 *Seismic Response and Reliability of Electrical Substation Equipment and Systems.* Junho Song, Armen Der Kiureghian, and Jerome L. Sackman. April 2006.

PEER 2005/15 *CPT-Based Probabilistic Assessment of Seismic Soil Liquefaction Initiation.* R. E. S. Moss, R. B. Seed, R. E. Kayen, J. P. Stewart, and A. Der Kiureghian. April 2006.

PEER 2005/14 *Workshop on Modeling of Nonlinear Cyclic Load-Deformation Behavior of Shallow Foundations.* Bruce L. Kutter, Geoffrey Martin, Tara Hutchinson, Chad Harden, Sivapalan Gajan, and Justin Phalen. March 2006.

PEER 2005/13 *Stochastic Characterization and Decision Bases under Time-Dependent Aftershock Risk in Performance-Based Earthquake Engineering.* Gee Liek Yeo and C. Allin Cornell. July 2005.

PEER 2005/12 *PEER Testbed Study on a Laboratory Building: Exercising Seismic Performance Assessment.* Mary C. Comerio, editor. November 2005.

PEER 2005/11 *Van Nuys Hotel Building Testbed Report: Exercising Seismic Performance Assessment.* Helmut Krawinkler, editor. October 2005.

PEER 2005/10 *First NEES/E-Defense Workshop on Collapse Simulation of Reinforced Concrete Building Structures.* September 2005.

PEER 2005/09 *Test Applications of Advanced Seismic Assessment Guidelines.* Joe Maffei, Karl Telleen, Danya Mohr, William Holmes, and Yuki Nakayama. August 2006.

PEER 2005/08 *Damage Accumulation in Lightly Confined Reinforced Concrete Bridge Columns.* R. Tyler Ranf, Jared M. Nelson, Zach Price, Marc O. Eberhard, and John F. Stanton. April 2006.

PEER 2005/07 *Experimental and Analytical Studies on the Seismic Response of Freestanding and Anchored Laboratory Equipment.* Dimitrios Konstantinidis and Nicos Makris. January 2005.

PEER 2005/06 *Global Collapse of Frame Structures under Seismic Excitations*. Luis F. Ibarra and Helmut Krawinkler. September 2005.

PEER 2005//05 *Performance Characterization of Bench- and Shelf-Mounted Equipment.* Samit Ray Chaudhuri and Tara C. Hutchinson. May 2006.

PEER 2005/04 *Numerical Modeling of the Nonlinear Cyclic Response of Shallow Foundations.* Chad Harden, Tara Hutchinson, Geoffrey R. Martin, and Bruce L. Kutter. August 2005.

PEER 2005/03 *A Taxonomy of Building Components for Performance-Based Earthquake Engineering.* Keith A. Porter. September 2005.

PEER 2005/02 *Fragility Basis for California Highway Overpass Bridge Seismic Decision Making*. Kevin R. Mackie and Božidar Stojadinović. June 2005.

PEER 2005/01 *Empirical Characterization of Site Conditions on Strong Ground Motion.* Jonathan P. Stewart, Yoojoong Choi, and Robert W. Graves. June 2005.

PEER 2004/09 *Electrical Substation Equipment Interaction: Experimental Rigid Conductor Studies.* Christopher Stearns and André Filiatrault. February 2005.

PEER 2004/08 *Seismic Qualification and Fragility Testing of Line Break 550-kV Disconnect Switches.* Shakhzod M. Takhirov, Gregory L. Fenves, and Eric Fujisaki. January 2005.

PEER 2004/07 *Ground Motions for Earthquake Simulator Qualification of Electrical Substation Equipment.* Shakhzod M. Takhirov, Gregory L. Fenves, Eric Fujisaki, and Don Clyde. January 2005.

PEER 2004/06 *Performance-Based Regulation and Regulatory Regimes.* Peter J. May and Chris Koski. September 2004.

PEER 2004/05 *Performance-Based Seismic Design Concepts and Implementation: Proceedings of an International Workshop.* Peter Fajfar and Helmut Krawinkler, editors. September 2004.

PEER 2004/04 *Seismic Performance of an Instrumented Tilt-up Wall Building.* James C. Anderson and Vitelmo V. Bertero. July 2004.

PEER 2004/03 *Evaluation and Application of Concrete Tilt-up Assessment Methodologies.* Timothy Graf and James O. Malley. October 2004.

PEER 2004/02 *Analytical Investigations of New Methods for Reducing Residual Displacements of Reinforced Concrete Bridge Columns.* Junichi Sakai and Stephen A. Mahin. August 2004.

PEER 2004/01 *Seismic Performance of Masonry Buildings and Design Implications.* Kerri Anne Taeko Tokoro, James C. Anderson, and Vitelmo V. Bertero. February 2004.

PEER 2003/18 *Performance Models for Flexural Damage in Reinforced Concrete Columns.* Michael Berry and Marc Eberhard. August 2003.

PEER 2003/17 *Predicting Earthquake Damage in Older Reinforced Concrete Beam-Column Joints.* Catherine Pagni and Laura Lowes. October 2004.

PEER 2003/16 *Seismic Demands for Performance-Based Design of Bridges.* Kevin Mackie and Božidar Stojadinović. August 2003.

PEER 2003/15 *Seismic Demands for Nondeteriorating Frame Structures and Their Dependence on Ground Motions.* Ricardo Antonio Medina and Helmut Krawinkler. May 2004.

PEER 2003/14 *Finite Element Reliability and Sensitivity Methods for Performance-Based Earthquake Engineering.* Terje Haukaas and Armen Der Kiureghian. April 2004.

PEER 2003/13 *Effects of Connection Hysteretic Degradation on the Seismic Behavior of Steel Moment-Resisting Frames.* Janise E. Rodgers and Stephen A. Mahin. March 2004.

PEER 2003/12 *Implementation Manual for the Seismic Protection of Laboratory Contents: Format and Case Studies.* William T. Holmes and Mary C. Comerio. October 2003.

PEER 2003/11 *Fifth U.S.-Japan Workshop on Performance-Based Earthquake Engineering Methodology for Reinforced Concrete Building Structures.* February 2004.

PEER 2003/10 *A Beam-Column Joint Model for Simulating the Earthquake Response of Reinforced Concrete Frames.* Laura N. Lowes, Nilanjan Mitra, and Arash Altoontash. February 2004.

PEER 2003/09 *Sequencing Repairs after an Earthquake: An Economic Approach.* Marco Casari and Simon J. Wilkie. April 2004.

PEER 2003/08 *A Technical Framework for Probability-Based Demand and Capacity Factor Design (DCFD) Seismic Formats.* Fatemeh Jalayer and C. Allin Cornell. November 2003.

PEER 2003/07 *Uncertainty Specification and Propagation for Loss Estimation Using FOSM Methods.* Jack W. Baker and C. Allin Cornell. September 2003.

PEER 2003/06 *Performance of Circular Reinforced Concrete Bridge Columns under Bidirectional Earthquake Loading.* Mahmoud M. Hachem, Stephen A. Mahin, and Jack P. Moehle. February 2003.

PEER 2003/05 *Response Assessment for Building-Specific Loss Estimation.* Eduardo Miranda and Shahram Taghavi. September 2003.

PEER 2003/04 *Experimental Assessment of Columns with Short Lap Splices Subjected to Cyclic Loads.* Murat Melek, John W. Wallace, and Joel Conte. April 2003.

PEER 2003/03 *Probabilistic Response Assessment for Building-Specific Loss Estimation.* Eduardo Miranda and Hesameddin Aslani. September 2003.

PEER 2003/02 *Software Framework for Collaborative Development of Nonlinear Dynamic Analysis Program.* Jun Peng and Kincho H. Law. September 2003.

PEER 2003/01 *Shake Table Tests and Analytical Studies on the Gravity Load Collapse of Reinforced Concrete Frames.* Kenneth John Elwood and Jack P. Moehle. November 2003.

PEER 2002/24 *Performance of Beam to Column Bridge Joints Subjected to a Large Velocity Pulse.* Natalie Gibson, André Filiatrault, and Scott A. Ashford. April 2002.

PEER 2002/23 *Effects of Large Velocity Pulses on Reinforced Concrete Bridge Columns.* Greg L. Orozco and Scott A. Ashford. April 2002.

PEER 2002/22 *Characterization of Large Velocity Pulses for Laboratory Testing.* Kenneth E. Cox and Scott A. Ashford. April 2002.

PEER 2002/21 *Fourth U.S.-Japan Workshop on Performance-Based Earthquake Engineering Methodology for Reinforced Concrete Building Structures.* December 2002.

PEER 2002/20 *Barriers to Adoption and Implementation of PBEE Innovations.* Peter J. May. August 2002.

PEER 2002/19 *Economic-Engineered Integrated Models for Earthquakes: Socioeconomic Impacts.* Peter Gordon, James E. Moore II, and Harry W. Richardson. July 2002.

PEER 2002/18 *Assessment of Reinforced Concrete Building Exterior Joints with Substandard Details.* Chris P. Pantelides, Jon Hansen, Justin Nadauld, and Lawrence D. Reaveley. May 2002.

PEER 2002/17 *Structural Characterization and Seismic Response Analysis of a Highway Overcrossing Equipped with Elastomeric Bearings and Fluid Dampers: A Case Study.* Nicos Makris and Jian Zhang. November 2002.

PEER 2002/16 *Estimation of Uncertainty in Geotechnical Properties for Performance-Based Earthquake Engineering.* Allen L. Jones, Steven L. Kramer, and Pedro Arduino. December 2002.

PEER 2002/15 *Seismic Behavior of Bridge Columns Subjected to Various Loading Patterns.* Asadollah Esmaeily-Gh. and Yan Xiao. December 2002.

PEER 2002/14 *Inelastic Seismic Response of Extended Pile Shaft Supported Bridge Structures.* T.C. Hutchinson, R.W. Boulanger, Y.H. Chai, and I.M. Idriss. December 2002.

PEER 2002/13 *Probabilistic Models and Fragility Estimates for Bridge Components and Systems.* Paolo Gardoni, Armen Der Kiureghian, and Khalid M. Mosalam. June 2002.

PEER 2002/12 *Effects of Fault Dip and Slip Rake on Near-Source Ground Motions: Why Chi-Chi Was a Relatively Mild M7.6 Earthquake.* Brad T. Aagaard, John F. Hall, and Thomas H. Heaton. December 2002.

PEER 2002/11 *Analytical and Experimental Study of Fiber-Reinforced Strip Isolators*. James M. Kelly and Shakhzod M. Takhirov. September 2002.

PEER 2002/10 *Centrifuge Modeling of Settlement and Lateral Spreading with Comparisons to Numerical Analyses***.** Sivapalan Gajan and Bruce L. Kutter. January 2003.

PEER 2002/09 *Documentation and Analysis of Field Case Histories of Seismic Compression during the 1994 Northridge, California, Earthquake.* Jonathan P. Stewart, Patrick M. Smith, Daniel H. Whang, and Jonathan D. Bray. October 2002.

PEER 2002/08 *Component Testing, Stability Analysis and Characterization of Buckling-Restrained Unbonded Braces™*. Cameron Black, Nicos Makris, and Ian Aiken. September 2002.

PEER 2002/07 *Seismic Performance of Pile-Wharf Connections.* Charles W. Roeder, Robert Graff, Jennifer Soderstrom, and Jun Han Yoo. December 2001.

PEER 2002/06 *The Use of Benefit-Cost Analysis for Evaluation of Performance-Based Earthquake Engineering Decisions*. Richard O. Zerbe and Anthony Falit-Baiamonte. September 2001.

PEER 2002/05 *Guidelines, Specifications, and Seismic Performance Characterization of Nonstructural Building Components and Equipment.* André Filiatrault, Constantin Christopoulos, and Christopher Stearns. September 2001.

PEER 2002/04 *Consortium of Organizations for Strong-Motion Observation Systems and the Pacific Earthquake Engineering Research Center Lifelines Program: Invited Workshop on Archiving and Web Dissemination of Geotechnical Data, 4–5 October 2001*. September 2002.

PEER 2002/03 *Investigation of Sensitivity of Building Loss Estimates to Major Uncertain Variables for the Van Nuys Testbed.* Keith A. Porter, James L. Beck, and Rustem V. Shaikhutdinov. August 2002.

PEER 2002/02 *The Third U.S.-Japan Workshop on Performance-Based Earthquake Engineering Methodology for Reinforced Concrete Building Structures*. July 2002.

PEER 2002/01 *Nonstructural Loss Estimation: The UC Berkeley Case Study.* Mary C. Comerio and John C. Stallmeyer. December 2001.

PEER 2001/16 *Statistics of SDF-System Estimate of Roof Displacement for Pushover Analysis of Buildings.* Anil K. Chopra, Rakesh K. Goel, and Chatpan Chintanapakdee. December 2001.

PEER 2001/15 *Damage to Bridges during the 2001 Nisqually Earthquake.* R. Tyler Ranf, Marc O. Eberhard, and Michael P. Berry. November 2001.

PEER 2001/14 *Rocking Response of Equipment Anchored to a Base Foundation.* Nicos Makris and Cameron J. Black. September 2001.

PEER 2001/13 *Modeling Soil Liquefaction Hazards for Performance-Based Earthquake Engineering.* Steven L. Kramer and Ahmed-W. Elgamal. February 2001.

PEER 2001/12 *Development of Geotechnical Capabilities in OpenSees.* Boris Jeremić. September 2001.

PEER 2001/11 *Analytical and Experimental Study of Fiber-Reinforced Elastomeric Isolators*. James M. Kelly and Shakhzod M. Takhirov. September 2001.

PEER 2001/10 *Amplification Factors for Spectral Acceleration in Active Regions.* Jonathan P. Stewart, Andrew H. Liu, Yoojoong Choi, and Mehmet B. Baturay. December 2001.

PEER 2001/09 *Ground Motion Evaluation Procedures for Performance-Based Design.* Jonathan P. Stewart, Shyh-Jeng Chiou, Jonathan D. Bray, Robert W. Graves, Paul G. Somerville, and Norman A. Abrahamson. September 2001.

PEER 2001/08 *Experimental and Computational Evaluation of Reinforced Concrete Bridge Beam-Column Connections for Seismic Performance.* Clay J. Naito, Jack P. Moehle, and Khalid M. Mosalam. November 2001.

PEER 2001/07 *The Rocking Spectrum and the Shortcomings of Design Guidelines.* Nicos Makris and Dimitrios Konstantinidis. August 2001.

PEER 2001/06 *Development of an Electrical Substation Equipment Performance Database for Evaluation of Equipment Fragilities.* Thalia Agnanos. April 1999.

PEER 2001/05 *Stiffness Analysis of Fiber-Reinforced Elastomeric Isolators.* Hsiang-Chuan Tsai and James M. Kelly. May 2001.

PEER 2001/04 *Organizational and Societal Considerations for Performance-Based Earthquake Engineering.* Peter J. May. April 2001.

PEER 2001/03 *A Modal Pushover Analysis Procedure to Estimate Seismic Demands for Buildings: Theory and Preliminary Evaluation.* Anil K. Chopra and Rakesh K. Goel. January 2001.

PEER 2001/02 *Seismic Response Analysis of Highway Overcrossings Including Soil-Structure Interaction.* Jian Zhang and Nicos Makris. March 2001.

PEER 2001/01 *Experimental Study of Large Seismic Steel Beam-to-Column Connections.* Egor P. Popov and Shakhzod M. Takhirov. November 2000.

PEER 2000/10 *The Second U.S.-Japan Workshop on Performance-Based Earthquake Engineering Methodology for Reinforced Concrete Building Structures.* March 2000.

PEER 2000/09 *Structural Engineering Reconnaissance of the August 17, 1999 Earthquake: Kocaeli (Izmit), Turkey.* Halil Sezen, Kenneth J. Elwood, Andrew S. Whittaker, Khalid Mosalam, John J. Wallace, and John F. Stanton. December 2000.

PEER 2000/08 *Behavior of Reinforced Concrete Bridge Columns Having Varying Aspect Ratios and Varying Lengths of Confinement.* Anthony J. Calderone, Dawn E. Lehman, and Jack P. Moehle. January 2001.

PEER 2000/07 *Cover-Plate and Flange-Plate Reinforced Steel Moment-Resisting Connections.* Taejin Kim, Andrew S. Whittaker, Amir S. Gilani, Vitelmo V. Bertero, and Shakhzod M. Takhirov. September 2000.

PEER 2000/06 *Seismic Evaluation and Analysis of 230-kV Disconnect Switches.* Amir S. J. Gilani, Andrew S. Whittaker, Gregory L. Fenves, Chun-Hao Chen, Henry Ho, and Eric Fujisaki. July 2000.

PEER 2000/05 *Performance-Based Evaluation of Exterior Reinforced Concrete Building Joints for Seismic Excitation.* Chandra Clyde, Chris P. Pantelides, and Lawrence D. Reaveley. July 2000.

PEER 2000/04 *An Evaluation of Seismic Energy Demand: An Attenuation Approach.* Chung-Che Chou and Chia-Ming Uang. July 1999.

PEER 2000/03 *Framing Earthquake Retrofitting Decisions: The Case of Hillside Homes in Los Angeles.* Detlof von Winterfeldt, Nels Roselund, and Alicia Kitsuse. March 2000.

PEER 2000/02 *U.S.-Japan Workshop on the Effects of Near-Field Earthquake Shaking.* Andrew Whittaker, ed. July 2000.

PEER 2000/01 *Further Studies on Seismic Interaction in Interconnected Electrical Substation Equipment.* Armen Der Kiureghian, Kee-Jeung Hong, and Jerome L. Sackman. November 1999.

PEER 1999/14 *Seismic Evaluation and Retrofit of 230-kV Porcelain Transformer Bushings.* Amir S. Gilani, Andrew S. Whittaker, Gregory L. Fenves, and Eric Fujisaki. December 1999.

PEER 1999/13 *Building Vulnerability Studies: Modeling and Evaluation of Tilt-up and Steel Reinforced Concrete Buildings.* John W. Wallace, Jonathan P. Stewart, and Andrew S. Whittaker, editors. December 1999.

PEER 1999/12 *Rehabilitation of Nonductile RC Frame Building Using Encasement Plates and Energy-Dissipating Devices.* Mehrdad Sasani, Vitelmo V. Bertero, James C. Anderson. December 1999.

PEER 1999/11 *Performance Evaluation Database for Concrete Bridge Components and Systems under Simulated Seismic Loads.* Yael D. Hose and Frieder Seible. November 1999.

PEER 1999/10 *U.S.-Japan Workshop on Performance-Based Earthquake Engineering Methodology for Reinforced Concrete Building Structures.* December 1999.

PEER 1999/09 *Performance Improvement of Long Period Building Structures Subjected to Severe Pulse-Type Ground Motions.* James C. Anderson, Vitelmo V. Bertero, and Raul Bertero. October 1999.

PEER 1999/08 *Envelopes for Seismic Response Vectors.* Charles Menun and Armen Der Kiureghian. July 1999.

PEER 1999/07 *Documentation of Strengths and Weaknesses of Current Computer Analysis Methods for Seismic Performance of Reinforced Concrete Members.* William F. Cofer. November 1999.

PEER 1999/06 *Rocking Response and Overturning of Anchored Equipment under Seismic Excitations.* Nicos Makris and Jian Zhang. November 1999.

PEER 1999/05 *Seismic Evaluation of 550 kV Porcelain Transformer Bushings.* Amir S. Gilani, Andrew S. Whittaker, Gregory L. Fenves, and Eric Fujisaki. October 1999.

PEER 1999/04 *Adoption and Enforcement of Earthquake Risk-Reduction Measures.* Peter J. May, Raymond J. Burby, T. Jens Feeley, and Robert Wood.

PEER 1999/03 *Task 3 Characterization of Site Response General Site Categories*. Adrian Rodriguez-Marek, Jonathan D. Bray, and Norman Abrahamson. February 1999.

PEER 1999/02 *Capacity-Demand-Diagram Methods for Estimating Seismic Deformation of Inelastic Structures: SDF Systems*. Anil K. Chopra and Rakesh Goel. April 1999.

PEER 1999/01 *Interaction in Interconnected Electrical Substation Equipment Subjected to Earthquake Ground Motions.* Armen Der Kiureghian, Jerome L. Sackman, and Kee-Jeung Hong. February 1999.

PEER 1998/08 *Behavior and Failure Analysis of a Multiple-Frame Highway Bridge in the 1994 Northridge Earthquake.* Gregory L. Fenves and Michael Ellery. December 1998.

PEER 1998/07 *Empirical Evaluation of Inertial Soil-Structure Interaction Effects.* Jonathan P. Stewart, Raymond B. Seed, and Gregory L. Fenves. November 1998.

PEER 1998/06 *Effect of Damping Mechanisms on the Response of Seismic Isolated Structures.* Nicos Makris and Shih-Po Chang. November 1998.

PEER 1998/05 *Rocking Response and Overturning of Equipment under Horizontal Pulse-Type Motions.* Nicos Makris and Yiannis Roussos. October 1998.

PEER 1998/04 *Pacific Earthquake Engineering Research Invitational Workshop Proceedings, May 14–15, 1998: Defining the Links between Planning, Policy Analysis, Economics and Earthquake Engineering.* Mary Comerio and Peter Gordon. September 1998.

PEER 1998/03 *Repair/Upgrade Procedures for Welded Beam to Column Connections.* James C. Anderson and Xiaojing Duan. May 1998.

PEER 1998/02 *Seismic Evaluation of 196 kV Porcelain Transformer Bushings.* Amir S. Gilani, Juan W. Chavez, Gregory L. Fenves, and Andrew S. Whittaker. May 1998.

PEER 1998/01 *Seismic Performance of Well-Confined Concrete Bridge Columns.* Dawn E. Lehman and Jack P. Moehle. December 2000.

ONLINE REPORTS

The following PEER reports are available by Internet only at http://peer.berkeley.edu/publications/peer_reports.html

PEER 2011/106 *Self Compacting Hybrid Fiber Reinforced Concrete Composites for Bridge Columns.* Pardeep Kumar, Gabriel Jen, William Trono, Marios Panagiotou, and Claudia Ostertag. September 2011.

PEER 2011/105 *Stochastic Dynamic Analysis of Bridges Subjected to Spacially Varying Ground Motions.* Katerina Konakli and Armen Der Kiureghian. August 2011.

PEER 2011/104 *Design and Instrumentation of the 2010 E-Defense Four-Story Reinforced Concrete and Post-Tensioned Concrete Buildings.* Takuya Nagae, Kenichi Tahara, Taizo Matsumori, Hitoshi Shiohara, Toshimi Kabeyasawa, Susumu Kono, Minehiro Nishiyama (Japanese Research Team) and John Wallace, Wassim Ghannoum, Jack Moehle, Richard Sause, Wesley Keller, Zeynep Tuna (U.S. Research Team). June 2011.

PEER 2011/103 *In-Situ Monitoring of the Force Output of Fluid Dampers: Experimental Investigation.* Dimitrios Konstantinidis, James M. Kelly, and Nicos Makris. April 2011.

PEER 2011/102 *Ground-motion prediction equations 1964 - 2010.* John Douglas. April 2011.

PEER 2011/101 *Report of the Eighth Planning Meeting of NEES/E-Defense Collaborative Research on Earthquake Engineering.* Convened by the Hyogo Earthquake Engineering Research Center (NIED), NEES Consortium, Inc. February 2011.

PEER 2010/111 *Modeling and Acceptance Criteria for Seismic Design and Analysis of Tall Buildings.* Task 7 Report for the Tall Buildings Initiative - Published jointly by the Applied Technology Council. October 2010.

PEER 2010/110 *Seismic Performance Assessment and Probabilistic Repair Cost Analysis of Precast Concrete Cladding Systems for Multistory Buildlings.* Jeffrey P. Hunt and Božidar Stojadinovic. November 2010.

PEER 2010/109 *Report of the Seventh Joint Planning Meeting of NEES/E-Defense Collaboration on Earthquake Engineering. Held at the E-Defense, Miki, and Shin-Kobe, Japan, September 18–19, 2009.* August 2010.

PEER 2010/108 *Probabilistic Tsunami Hazard in California.* Hong Kie Thio, Paul Somerville, and Jascha Polet, preparers. October 2010.

PEER 2010/107 *Performance and Reliability of Exposed Column Base Plate Connections for Steel Moment-Resisting Frames.* Ady Aviram, Božidar Stojadinovic, and Armen Der Kiureghian. August 2010.

PEER 2010/106 *Verification of Probabilistic Seismic Hazard Analysis Computer Programs.* Patricia Thomas, Ivan Wong, and Norman Abrahamson. May 2010.

PEER 2010/105 *Structural Engineering Reconnaissance of the April 6, 2009, Abruzzo, Italy, Earthquake, and Lessons Learned.* M. Selim Günay and Khalid M. Mosalam. April 2010.

PEER 2010/104 *Simulating the Inelastic Seismic Behavior of Steel Braced Frames, Including the Effects of Low-Cycle Fatigue.* Yuli Huang and Stephen A. Mahin. April 2010.

PEER 2010/103 *Post-Earthquake Traffic Capacity of Modern Bridges in California.* Vesna Terzic and Božidar Stojadinović. March 2010.

PEER 2010/102 *Analysis of Cumulative Absolute Velocity (CAV) and JMA Instrumental Seismic Intensity (I_{JMA}) Using the PEER–NGA Strong Motion Database.* Kenneth W. Campbell and Yousef Bozorgnia. February 2010.

PEER 2010/101 *Rocking Response of Bridges on Shallow Foundations.* Jose A. Ugalde, Bruce L. Kutter, and Boris Jeremic. April 2010.

PEER 2009/109 *Simulation and Performance-Based Earthquake Engineering Assessment of Self-Centering Post-Tensioned Concrete Bridge Systems.* Won K. Lee and Sarah L. Billington. December 2009.

PEER 2009/108 *PEER Lifelines Geotechnical Virtual Data Center.* J. Carl Stepp, Daniel J. Ponti, Loren L. Turner, Jennifer N. Swift, Sean Devlin, Yang Zhu, Jean Benoit, and John Bobbitt. September 2009.

PEER 2009/107 *Experimental and Computational Evaluation of Current and Innovative In-Span Hinge Details in Reinforced Concrete Box-Girder Bridges: Part 2: Post-Test Analysis and Design Recommendations.* Matias A. Hube and Khalid M. Mosalam. December 2009.

PEER 2009/106 *Shear Strength Models of Exterior Beam-Column Joints without Transverse Reinforcement.* Sangjoon Park and Khalid M. Mosalam. November 2009.

PEER 2009/105 *Reduced Uncertainty of Ground Motion Prediction Equations through Bayesian Variance Analysis.* Robb Eric S. Moss. November 2009.

PEER 2009/104 *Advanced Implementation of Hybrid Simulation.* Andreas H. Schellenberg, Stephen A. Mahin, Gregory L. Fenves. November 2009.

PEER 2009/103 *Performance Evaluation of Innovative Steel Braced Frames.* T. Y. Yang, Jack P. Moehle, and Božidar Stojadinovic. August 2009.

PEER 2009/102 *Reinvestigation of Liquefaction and Nonliquefaction Case Histories from the 1976 Tangshan Earthquake.* Robb Eric Moss, Robert E. Kayen, Liyuan Tong, Songyu Liu, Guojun Cai, and Jiaer Wu. August 2009.

PEER 2009/101 *Report of the First Joint Planning Meeting for the Second Phase of NEES/E-Defense Collaborative Research on Earthquake Engineering.* Stephen A. Mahin et al. July 2009.

PEER 2008/104 *Experimental and Analytical Study of the Seismic Performance of Retaining Structures.* Linda Al Atik and Nicholas Sitar. January 2009.

PEER 2008/103 *Experimental and Computational Evaluation of Current and Innovative In-Span Hinge Details in Reinforced Concrete Box-Girder Bridges. Part 1: Experimental Findings and Pre-Test Analysis.* Matias A. Hube and Khalid M. Mosalam. January 2009.

PEER 2008/102 *Modeling of Unreinforced Masonry Infill Walls Considering In-Plane and Out-of-Plane Interaction.* Stephen Kadysiewski and Khalid M. Mosalam. January 2009.

PEER 2008/101 *Seismic Performance Objectives for Tall Buildings.* William T. Holmes, Charles Kircher, William Petak, and Nabih Youssef. August 2008.

PEER 2007/101 *Generalized Hybrid Simulation Framework for Structural Systems Subjected to Seismic Loading.* Tarek Elkhoraibi and Khalid M. Mosalam. July 2007.

PEER 2007/100 *Seismic Evaluation of Reinforced Concrete Buildings Including Effects of Masonry Infill Walls.* Alidad Hashemi and Khalid M. Mosalam. July 2007.

The Pacific Earthquake Engineering Research Center (PEER) is a multi-institutional research and education center with headquarters at the University of California, Berkeley. Investigators from over 20 universities, several consulting companies, and researchers at various state and federal government agencies contribute to research programs focused on performance-based earthquake engineering.

These research programs aim to identify and reduce the risks from major earthquakes to life safety and to the economy by including research in a wide variety of disciplines including structural and geotechnical engineering, geology/seismology, lifelines, transportation, architecture, economics, risk management, and public policy.

PEER is supported by federal, state, local, and regional agencies, together with industry partners.

PEER reports can be ordered at http://peer.berkeley.edu/publications/peer_reports.html or by contacting

Pacific Earthquake Engineering Research Center
University of California, Berkeley
325 Davis Hall, mail code 1792
Berkeley, CA 94720-1792
Tel: 510-642-3437
Fax: 510-642-1655
Email: peer_editor@berkeley.edu

ISSN 1547-0587X